5-2018

Using Remotely Piloted Aircraft and Infrared Technology to Detect and Monitor Greater Sage-Grouse

Thomas R. Thompson
Utah State University

USING REMOTELY PIOLTED AIRCRAFT AND INFARED TECHNOLOGY TO DETECT AND MONITOR GREATER SAGE-GROUSE

by

Thomas R. Thompson

A thesis submitted in partial fulfillment
of the requirements for the degree

of

MASTER OF SCIENCE

in

Ecology

Approved:

_____	_____
R. Douglas Ramsey Major Professor	Terry A. Mesmer Committee Member
_____	_____
Eugene W. Schupp Committee Member	Mark R. McLellan Vice President for Research and Dean of the School of Graduate Studies

UTAH STATE UNIVERSITY
Logan, Utah

2018

ABSTRACT

Using Remotely Piloted Aircraft to Detect and Monitor Greater Sage-grouse

by

Thomas R. Thompson, Master of Science

Utah State University, 2018

Major Professor: Dr. R. Douglas Ramsey
Department: Wildland Resources

In wildlife management, using cutting edge technology and science to monitor greater sage-grouse (*Centrocercus urophasianus; sage-grouse*) populations enable land managers to better assess the impact of management decisions. Following a traditional method of conducting a sage-grouse census by monitoring an active lek during breeding season, we used a remotely piloted aircraft (RPA) equipped with a thermal camera to determine its potential to detect, monitor, and classify sage-grouse by sex. In total, we conducted six flights over a six-week period, five of which occurred during the early morning at sunrise (0650 in UTC-6) and used an RPA coupled with a high resolution thermal infrared camera to capture thermal infrared video. The sixth flight was conducted at mid-afternoon using a traditional RGB camera to collect visible color photography and create a 1cm resolution orthomosaic of the lek. Still image frames were extracted from the thermal video and sage-grouse observations were mapped onto the 1cm orthomosaic along with attribute data documenting their physical characteristics.

The 1cm resolution base map increased our confidence in the manual placement of sage-grouse locations. We were able to extract physical characteristics of sage-grouse individuals (i.e., length and size), as well as thermal responses (maximum, minimum, and mean temperature)) from the thermal imagery which enabled us to identify gender and activity of males (displaying or non-displaying.) This process also allowed us to create a digital archive of sage-grouse locations along with their physical characteristics. Combining the five thermal flights, we identified an average of 4.4 displaying males, 13.4 non-displaying males, and 5.6 female sage-grouse per flight, and cataloged the geographic location and anatomical characteristics of all 117 bird observations across all flights. We found that thermal characteristics between displaying males, non-displaying males, and females differed, indicating that this technique can effectively identify gender and activity of sage-grouse occupying a lek.

(100 pages)

PUBLIC ABSTRACT

Using Remotely Piloted Aircraft to Detect and Monitor Greater Sage-Grouse

Thomas R. Thompson

In wildlife management, using cutting edge technology and science to monitor greater sage-grouse (*Centrocercus urophasianus; sage-grouse*) populations, enables land managers to better assess the impact of their management decisions. Having precise counts of sage-grouse lek attendance, and specifically male lek attendance, is an important metric used to evaluate population status and response to conservation actions (Gifford et.al, 2013, Dahlgren et al., 2016). Leks are seasonal breeding sites where males perform a ritualistic courtship dance for females.

Our case study examined if a Remotely Piloted Aircraft (RPA) was effective in detecting, and counting, sage-grouse during the lek season (early March to late April). More specifically, this research used a Forward-Looking Infrared (FLIR) camera (a thermal camera) to detect sage-grouse and determine body temperatures of individual sage-grouse to determine if temperature data can be used to identify displaying male sage-grouse. These images can be used to document the activity and behavior of sage-grouse and can be revisited at future times to document changes in bird numbers as well as perform additional statistical analyses.

We conducted 5 flights and on a per-flight basis, we identified an average of 4.4 displaying males, 13.4 non-displaying males, and 5.6 female sage-grouse. We found that the average size and average maximum temperature of the three sage-grouse categories

differed where females were smaller with an average body size of 325cm^2, an average maximum temperature of 14.6 C˚, and a smaller average thermal range of 2.47 C˚. Non-displaying male body size was approximately 488cm^2, with a maximum average temperature of 17.2 C˚, and an average thermal range of 4.66C˚. Displaying male body size was the largest at approximately 655cm^2, an average maximum temperature of 27.5 C˚, with the largest average range of 12.39C˚. Our study demonstrates that RPA and infrared technology can be used to conduct accurate sage-grouse lek attendance counts. Further, results of this study will also provide a guideline for the use of RPA's to monitor sage-grouse and other lekking species.

DEDICATION

To my inspirational, beautiful, and loving wife Tiffany; to my mentors, friends, family, and my children yet to come.

ACKNOWLEDGMENTS

While I have many people to be thankful for in my life, I would like to start by acknowledging my professor Dr. R. Douglas Ramsey. I am extremely grateful for having the opportunity to work with a professor who allowed me to barge into his office with questions regarding my professional and academic work. He was not only my academic mentor and advisor but he also acted as a personal advisor and friend on more than just a few occasions. The two most memorable times he demonstrated his high regard for me, was when he and his wife came to the surprise engagement party I threw for my wife. The second time was when he and his wife attended my wedding. I will never forget the lessons he has taught me both academically and professionally. Nor will I forget the personal and financial investments he made in me, which propelled me to my personal and academic success.

I also want to express my gratitude to my other committee members, Eugene "Geno" Schupp and Terry Messmer. One of the first unforgettable courses I took at USU was an exceptional undergraduate Ecology class taught by Geno. He has also offered important input to my thesis. I want to thank Terry for being willing to be on my committee and for his valuable comments on my thesis project ideas and for the feedback on my work. He has also offered valuable connections, papers, and insights to the legal navigation of conducting studies with wildlife and domestic animals.

The "honorary committee members" and advisors that I would like to mention is the team of professionals found in the RS/GIS Lab (Chris and Ellie McGinty, Chris Garrard, Alexander Hernandez, and Ben Crabb). Each one of these people have gone

from being colleagues to friends who are genuinely happy to see each other succeed and overcome adversity. In one way or another each and every one of these kind, generous, and intelligent people gave me the moral and professional support that comes from friends rather than someone who is simply a co-worker. I have worked diligently to get where I am professionally, but I also realize that I would not be as academically and professionally successful without the influences of these individuals as my foundation to that success. I hope that everyone who has contributed to my thesis can, in some way, see our ideas come to fruition through the writing found in this document.

I need to also express my gratitude to Brad Hunt and his staff at Hardware Ranch for the permission to access the wildlife management area on several occasions. I also want to thank Avery Cook for initially meeting at the beginning of this research project to give his professional insight. He helped in filing proper paper work with the Division of Wildlife Resources needed for the completion of this project.

I would like to give special thanks to each and every one of my family, friends, and acquaintances who have provided their positive influences and moral support. As I have worked through some incredibly difficult parts of my life, these people have always stood by my side and helped me when I needed support. I would like to particularly thank my loving parents and siblings for encouraging me to attend graduate school and for believing in my ability to be where I am today. I want to especially thank them for being patient with me over the last few months of my graduate degree and for the boundless love and support they provide to me.

Finally, I want to thank my wife. Tiffany has lifted me up when I was down and

encouraged me on the days where she witnessed me struggle most. I can never thank her enough for choosing me as a partner in life.

Thomas R. Thompson

CONTENTS

Page

LIST OF TABLES

LIST OF FIGURES

INTRODUCTION

Currently, greater sage-grouse (*Centrocercus urophasianus*; sage-grouse) are considered "not-warranted" for listing under the United States Endangered Species Act of 1973 (ESA 1973, as amended), with a five year review of the decision scheduled for September 2020 (Department of Interior & Fish and Wildlife Service 2015). This decision was primarily due to federal and state conservation plans and efforts currently being applied by individual states (Doherty et al. 2016). It is therefore important to monitor sage-grouse populations to assess impacts of management decisions and thus the success of management plans. Since 2010, stakeholders participating in the Sage-Grouse Initiative have invested $424.5 million dollars to conserve 4.4 million acres on property held by more than 1,100 landowners (Opar 2015). Some refer to sage-grouse as an umbrella species for sagebrush rangelands. By protecting them as a species, there are indirect protections applied to other species in the ecological communities making up sage-grouse habitat (Knick et al. 2013). Sage-grouse populations provide qualitative assessments regarding the health of sagebrush ecosystems and rangelands in general (Rowland et al. 2006).

Land managers and wildlife biologists use population counts of male sage-grouse as an important metric to help determine the size and health of sage-grouse populations (Gillette et al. 2013, Dahlgren et al. 2016). Previous research has shown that it is unlikely that all male sage-grouse are detected during lek counts, which complicates the use of lek counts as an index to estimate population abundance Fremgen et al. (2016). As described by Guttery et al. (2013), in the absence of validated sex ratios, wildlife

management agencies adopt conservative assumption that the breeding season sex ratio is at a parity of (1:1) to avoid the possibility of overestimating population size, which may contribute to the failure to identify the vital rates that affect population growth (Dahlgren et al. 2016). In adopting conservative estimates and knowing it is unlikely that all male sage-grouse are being detected, there is need for better tools and methods to document all sage-grouse individuals (male and female) occupying a lek. An active lek is described by Connelly et al. 2003, as a geographic area where males traditionally gather, occurring within two or more of the previous five years, to engage in competitive displays to entice prospective females for copulation. Leks are normally located in open areas with low vegetation cover, typically adjacent to sagebrush-dominated landscapes.

Our study expands current and accepted field techniques used by land managers to count sage grouse and document annual male lek attendance that can be utilized for population modeling such as those found in Johnson and Rowland (2007), Connelly and Schroeder (2007) and Blomberg et al. (2013). Our proof of concept study examines the use of remotely piloted aircraft (RPA) and thermal videography (thermography) as a potential tool to census individual male and female sage-grouse to estimate population abundance at a lek. This study demonstrates that RPA's, accompanied with an infrared camera, are effective tools for accurately mapping the spatial distribution of sage-grouse individuals as well as determining the sex of individual birds using their thermal signatures (maximum, minimum, and mean temperatures).

By utilizing recent advances in technology, we now have the ability to capture radiometrically calibrated thermal infrared aerial imagery of sage-grouse leks that

effectively creates a permanent record of activity within a lek and can therefore be used for further analysis in the future (Hartmann et al. 2012, Gillette et al. 2013, Gillette et al. 2015, Hanson et al. 2014, Stark et al. 2014). In comparison to wildlife surveys using traditional manned aircraft, RPA can be more affordable and applicable at smaller scales (Jones et al. 2006). For example, a single wildlife management area could be covered by a RPA which may be too costly or too impractical for traditional manned aircraft (Jones et al. 2006). RPA provide multiple benefits particularly in terms of cost, safety and low impact on wildlife communities (Jones and Rowland 2006, Hanson et al. 2014, Martin 2014). Current field techniques used to count lek attendance by male sage-grouse, regardless of accuracy, can never be truly revisited by another researcher (Hanson et al. 2014). An image-based technique, however, serves as a permanent record of field conditions, ecological communities, and sage-grouse locations at the time of image acquisition. This permanent field record can be revisited by others at any time and as many times needed to ensure every single bird is detected, monitored, and categorized. By using a multi-rotor RPA compared to a fixed-wing manned or unmanned platform, we provide insight into how a slower and lower flying data collection platform can perform in this task. This is a technique that has little representation in the literature. As in many wildlife research and management disciplines, it is important to have tools that are precise, non-invasive, and cost-effective(Martin 2014).

While the legitimacy of using a lek census as an accurate metric to estimate population size is rarely disputed (Johnson and Rowland 2007, Connelly and Schroeder 2007). One portion of this study focuses on the accepted techniques of ground counting

male sage-grouse during the spring lek season. In our study, a traditional ground count of sage-grouse was done minutes before launching the RPA to conduct the aerial census to compare the difference between methodologies. Spring counts of males on leks are considered the most reliable survey method for predicting population growth (Connelly et al. 2003 and Connelly and Schroeder 2007). By using a multi rotor RPA we hope to eliminate the error introduced by convenience sampling (Johnson and Rowland 2007) where accessibility to leks may impact the accuracy of population estimates and bias inferences. Connelly et al. (2003), Johnson and Rowland (2007) stated that although sage-grouse on leks can be counted from the air using natural color photography or visually at the time of the flight, such counts are difficult and rarely as accurate as ground counts. Further, conducting aerial surveys from manned aircraft involve inherent risks to the pilot and crew when flying at 100m to 150m above ground level. Using traditional manned aircraft can be more expensive and potentially more invasive to wildlife species when compared to RPA (Martin 2014). Advances in both RPA platforms (multi-rotor and fixed-winged) and thermal infrared sensors have resulted in a more effective and cost efficient method as compared to conventional manned aircraft (Rango et al. 2006).

Sage-grouse conservation efforts are guided by population estimation and monitoring using lek-based survey methods (Gillette et al. 2013, Dahlgren et al. 2016). Using technology such as RPA and thermography, land managers can collect, archive, and revisit digital imagery and videos to better evaluate sage-grouse population trends. Our study aids in determining if a unique data set can be produced by an RPA and infrared camera that can then be shared and leveraged by others within the scientific and

management communities.

The use of remotely piloted aircraft for wildlife research has increased (Martin 2014). The use of RPAs for wildlife research and management may provide a safer and more cost-effective method as compared to conventionally manned aircraft (Rango et al. 2006). Furthermore, the ability to quickly mobilize and collect data at any location surpasses conventional aircraft that require more lead-time, are more expensive, and cannot fly at low altitudes (Rango et al. 2006).

Our study builds on past studies such as Hanson et al. (2014) which used a thermal and a visible camera mounted to a Raven RQ-11 fixed-wing RPA manufactured by AreoVironment©, as well as a study conducted by Gillette et al. 2015 which used a Maule 7-235 fixed-wing manned aerial platform and a Mid-wav infrared RS67000 gyro stabilized camera. Our study is unique in that we are utilizing a hovering RPA and evaluating the ability of a thermal infrared camera to differentiate the thermal properties of displaying males, non-displaying males, and females. The hypothesis for this study is that displaying adult male sage-grouse have a unique thermal signature, when compared to non-displaying males and females due to the inflation of the apteria (a fleshy patch of skin) on the breast of adult male sage-grouse.

To the best of our knowledge, there has not been any research conducted utilizing a multi rotor RPA and an uncooled microbolometer (micro-sensor array) thermal infrared sensor to count sage-grouse on a lek and to use the thermal response to determine sex morphologies and activity of sage-grouse individuals. Our research goals were to determine if a) sage-grouse can be counted using a thermal camera mounted to a vertical

take-off and landing (VTOL) RPA, b) sage-grouse sex morphologies and behavior within a lek can be determined using a thermal camera, and c) the presence of the hovering RPA affects sage-grouse behavior.

The greater sage-grouse

The greater sage-grouse is the largest grouse species in North America. The backs and wings of both male and female sage-grouse are mottled gray and brown with bodies that are black with speckles of white. The male sage-grouse has a black throat and a fully white chest with a long, pointed tail that opens up in a fan-like manner during display. Males also have fleshy yellow combs over the eyes, phylloplumes located at the back of the head and neck, and white feathers forming a ruff around the neck and upper

Figure 1. Anatomical difference between a displaying male (on the right) and female (on the left) sage-grouse (*Centrocercus urophasianus*). Displaying males have unique fleshy patches between feathered areas on the chest (apteria). Male sage-grouse expose these fleshy patches of skin during the ritualistic displaying behavior when attempting to entice prospective females for copulation. Photo source and location: Dr. R. Douglas Ramsey April, 2016 located on Hardware Ranch Wildlife Management Area (HWRWMA) study site.

belly. Adult males vary in length from 66 to 76cm and weighs between 2 and 3kg. The adult females are smaller, ranging in length from 48 to 58cm and weighing between 1 and 2kg (Hartmann et al. 2012, Casana et al. 2017). The most unique difference between males and females is that during breeding displays, males will inflate and deflate olive-green bare flesh patches of skin (more formally referred to as apteria) on their chests (Department of Interior & Fish and Wildlife Service 2010) (Figure 1).

The apteria and yellow eyebrow combs are distinctly unique to male sage-grouse. Figure 1 shows the anatomical differences between a displaying male and female sage-grouse. During the lekking season and just before sunrise, males move onto the lek to display for females. The morning is conveniently the daily thermal inertia minimum for land surfaces, creating contrast between sage-grouse bodies against the background of vegetation, soil, and snow. These environmental and anatomical parameters make it relatively simple to identify individual birds.

Thermal characteristics of greater sage-grouse

Thermal radiation is the emission of electromagnetic energy away from a given object. Typically, this emitted radiation is not visible to humans except when an object is "red hot" and the emitted EM energy is predominantly composed of the visible red (~0.62 – 0.75 microns) portion of the spectrum. Surfaces that are generally cool to the touch emit EM radiation predominantly in the non-visible portion of the spectrum. For instance, the human body at 98.6 ˚F (37 ˚C) has a peak EM emittance at 9.3 microns and the Earth (at an average temperature of 16 ˚C) has a peak emittance of 10 microns. The portion of the EM spectrum that we commonly refer to as the thermal infrared region

ranges from about 8-15 microns. This is the portion of the EM spectrum where most surface features on earth emit peak radiation depending on temperature.

A governing relationship of radiant heat energy follows the Stefan-Boltzmann law which states that the total radiant heat energy of a surface is proportional to the fourth power of its temperature measured in Kelvin (R = T^4). The rate at which energy leaves an object is explained by the Stefan-Boltzmann Equation given as $\frac{\Delta Q}{\Delta t} = \in \delta A T^4$ where Q is energy and t is time. The change in energy per unit time is equal to the product of emissivity ($\in$), the Stefan-Boltzmann constant (δ), area (A), and temperature (T) in Kelvin. The Stefan-Boltzmann Constant is given as: $= 5.67 * 10^{-8} \frac{Watts}{meters^2 * Kelvin^4}$. The emissivity of an object is defined by the objects proportional effectiveness in emitting energy as compared to a black body and ranges from 0 to 1. If an object is made up of a very black surface, it will have an emissivity close to 1 and radiate heat efficiently. Conversely, a white or shiny surface will have an emissivity close to 0 implying that it will radiate heat poorly. An object that radiates energy well also absorbs energy well and an object that radiates poorly also absorbs poorly (Blevin and Brown 1971).

In principle, aerial thermal imaging is relatively simple. Different materials and their varying compositions will absorb, emit, transmit, and reflect radiation at different rates (Casana et al. 2017). Thermal infrared cameras are sensitive to that portion of the EM spectrum that is generally emitted by different materials.

STUDY SITE

The study area is located on the Hardware Ranch Wildlife Management Area (HWRWMA) in northern Utah. The management area is located in Blacksmith Fork canyon about 15 miles east of Hyrum, Utah, on state road 101. The land is owned by the State of Utah and is managed by the Utah Division of Wildlife Resources who provided access to the lek. The HWRWMA is managed primarily for big game wildlife such as deer, elk, and moose. The property also supports two active sage-grouse leks. The lek

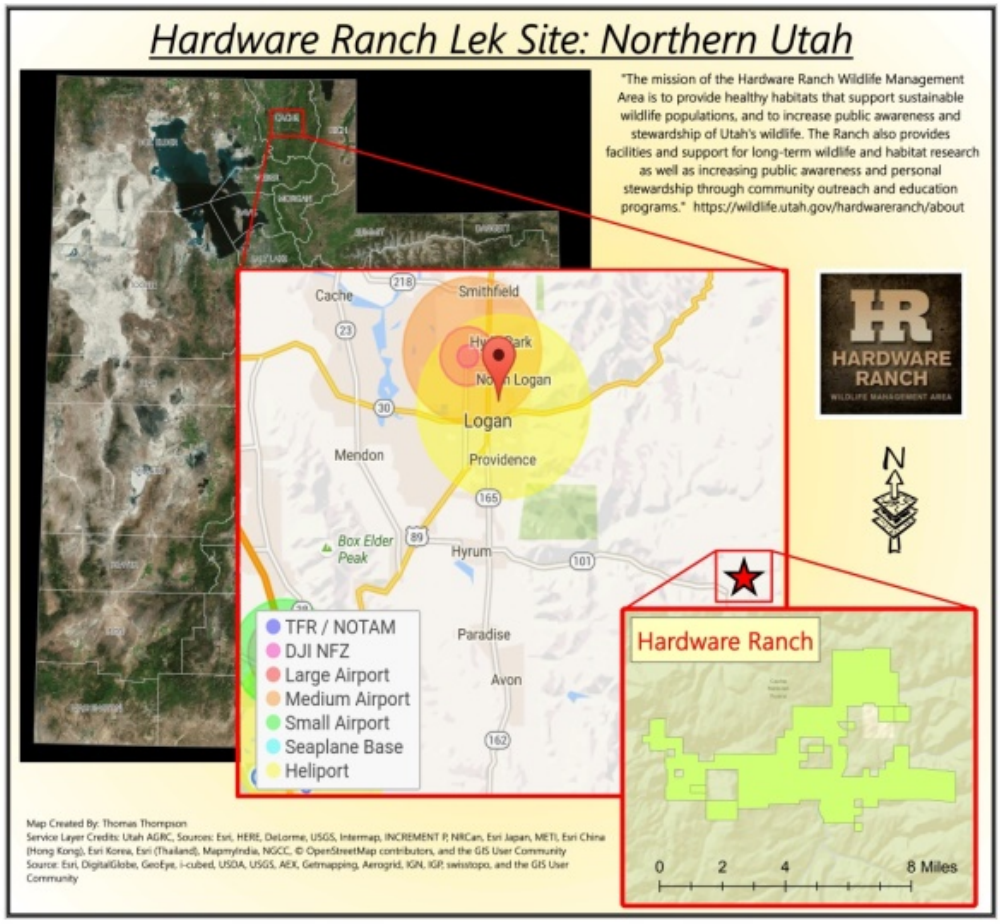

Figure 2. The study area is located in northern Utah on the Hardware Ranch Wildlife Management Area (HWRWMA). The property is owned by the State of Utah and is managed by the Utah Division of Wildlife Resources. The middle-inset map identifies local No-Fly Zone.

used for this study was identified with the assistance of the Hardware Ranch Manager (Figure 2). There are three small bodies of water on or near the lek site. These are small earthen impoundments, one of which is located adjacent to the lek (Figure 3). The elevation of the study site ranges from 1724.72 meters to 1746.24 meters (Figure 4).

Hardware Ranch has an annual average total precipitation of 205.4 cm, where the majority of the precipitation (162cm) comes in the form of snow (WRCC 2006). The annual average maximum temperature is 15 C˚ (59.1 F) and the annual average minimum is -4.8 C˚ (23.4 F). The vegetation types surrounding the lek consist primarily of Mountain Big Sagebrush (*A. tridentata spp vaseyana*) and Bluebunch Wheatgrass (*Pseudorogeneria spicata*), as well as an assortment of other montane grasses and forbs (Figure 5).

Figure 3. Ultra-High Resolution image map of the study site where greater sage-grouse *(Centrocercus urophasianus*) were monitored between March 5, 2016 and April 5, 2016.

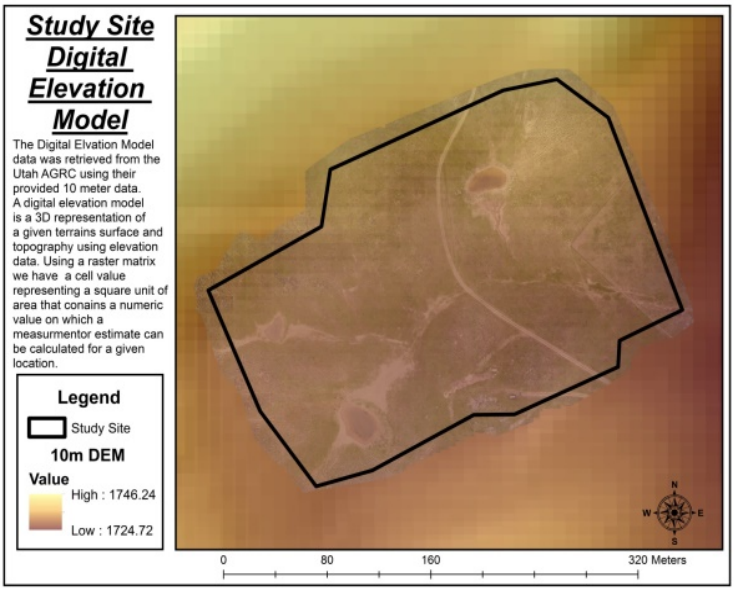

Figure 4. Map of the lek site showing a 10m resolution digital elevation model (DEM) provided by the Automated Geographic Reference Center (AGRC). The black polygon represents the study site area and the dark brown pixels represent the lowest topographic regions of the lek. The lightest yellow pixels represent the highest topographic regions of the sage-grouse lek.

Figure 5. Images of typical ground cover surrounding the lek including mountain big sagebrush, grasses and forbs. Ground control points (GCP) were used to aid in geo-referencing thermal imagery and sage-grouse locations captured during the remotely piloted aircrafts (RPA) aerial census. . Photo source and location: Thomas Thompson April, 2016. Located on Hardware Ranch Wildlife Management Area (HWRWMA) study site.

The soil is a mountain stony loam, moderately deep, well drained, and non-saline (U.S. Department of Agriculture & Natural Resource Conservation Service 2012). Soils are developed from colluvium, alluvium, and residuum from surrounding hills and mountains. The permeability of the soil is moderately slow with available water holding capacity between 5.33 cm to 12.44 cm (2.1 to 4.9 inches) in the upper 101.6 cm (40 inches) of soil. The soil in and around the lek is classified as a mollisol with a xeric soil moisture regime and a temperature regime that is best classified as frigid, ranging from ~0˚ C to 8˚ C ("SoilWeb: An Online Soil Survey Browser | California Soil Resource Lab," 2016).

A 10m resolution digital elevation model produced by the U.S. Geological Survey and acquired from the Utah Automated Geographic Reference Center (AGRC) was used to calculate percent slope and slope aspect of the study site using the ArcMap™ Spatial Analyst tool. The slope aspect (Figure 6) showed that the lek itself is generally south facing with some portions of the lek facing to the southeast and southwest. On the far south side of the lek, slopes predominantly face north and east with some northeast and northwest facing slopes (Figure 7). The slope raster showed that the majority of the lek is relatively flat (green and light green pixels represent areas with low slope percent values), with steeper topography on the western, northern, and eastern edges (steepest topographical features are seen in red in Figure 7).

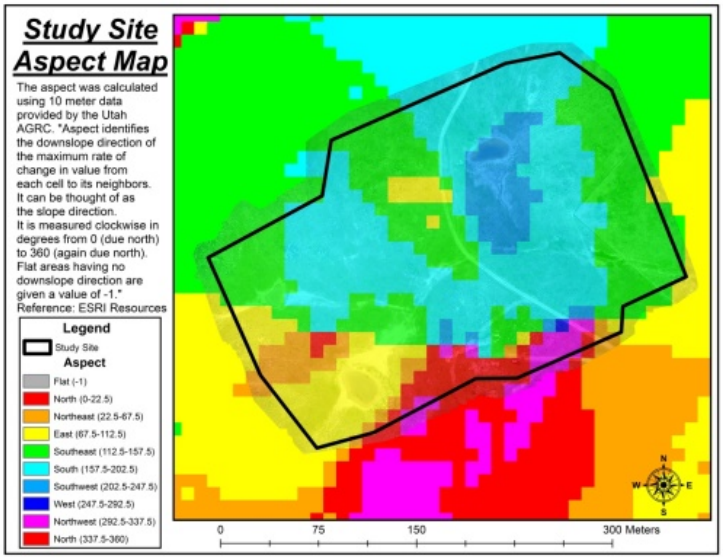

Figure 6. Slope aspect map was produced using a 10m digital elevation model (DEM) provided by the Automated Geographic Reference Center (AGRC). The aspect map identified the majority of the lek is south (teal pixels), southeast (green pixels), and south west facing (blue pixels) slopes. The southern portion of the aspect map depicted the majority of the north facing and east facing slopes

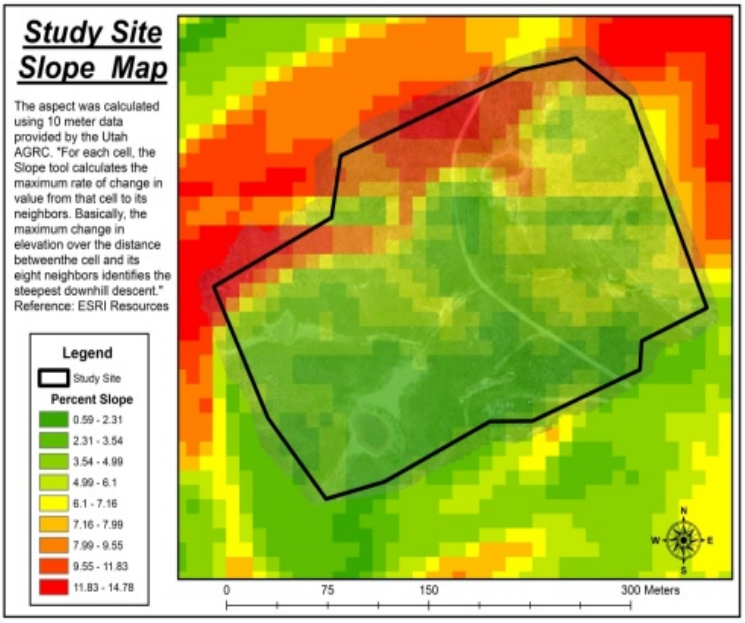

Figure 7. Slope map was calculated using a 10m digital elevation model (DEM) provided by the Automated Geographic center (AGRC). While there is a 20m difference in elevation in the study site, the slope map shows that the majority of the study site has very little slope (green and light green pixels) and is relatively flat. The red and orange pixels represent the areas of the study area where the highest percent of slope can be found.

METHODS

Data collection and processing

The RPA used in this study is the DJI-S1000 (manufactured by Da-jiang Innovations Science and Technology Col, Ltd headquartered in Shenzhen Guangdong), a portable, high-payload capacity octo-rotor aircraft. This platform was fitted with a custom 3D-printed box designed to carry the thermal camera payload. The content of the payload container included an Asus vivo minicomputer, a Goal Zero Sherpa 50 power pack (manufactured by Goal Zero located in South Bluffdale, UT, USA), and two cameras. The first camera is a Sony A7r 36.4 megapixel full-frame mirrorless digital camera (Manufactured by Sony corporation headquarters are in Konan, Minato, Tokyo) with the Sony Sonnar T* anti-reflective, FE35mm, F/2.8 ZA 35mm lens with a horizontal field of view of 54˚. The second sensor is a forward-looking infrared (FLIR) thermal infrared (TIR) imaging camera (manufactured by FLIR Systems headquartered in Wilsonville, OR) – the FLIR A65sc is sensitive to electromagnetic spectrum wavelengths between 7.5-13 microns. This is an uncooled VOX microbolometer detector with a resolution of 640 x 512. The thermal camera was fitted with a 25mm lens which has a 25˚ horizontal and 20˚ vertical field of view. The FLIR thermal camera is capable of collecting 327,680 pixels per frame and records video at a 30hz image frequency with a thermal sensitivity of +/- 0.05 ˚C, and an absolute accuracy of +/- 5 ˚C.

Data processing used Pix4Dmapper Pro to automate the digital photogrammetric process and create the natural color orthomosaic base map using a process often referred to as Structure from Motion (SFM)(Hartmann et al. 2012, Casana et al. 2017). Data

processing also included FLIR ResearchIR software to convert the radiometric measurements collected by the FLIR A65sc and convert them to temperature in ˚C.

Image acquisition

The DJI s1000+ octocopter with the custom 3D printed payload box mounted to the bottom is displayed in Figure 8. Thermal video imagery was collected by the FLIR A65sc camera at a rate of 30 frames per second. For the final afternoon flight, the system carried the Sony A7r natural color camera with an on-camera intervelometer set to capture images at one frame every two seconds.

Figure 8. DJI S1000+ carrying the thermal and visible light cameras.

Since this study included an interaction with live animals (sage-grouse), approval for the study was sought and granted from the Institutional Animal Care and Use Committee at Utah State University (IACUC#2570). Further, since data collection occurred over land managed directly by the Utah Division of Wildlife Resources (UDWR) and with a species of concern, permission was sought from and granted by the UDWR (COR #2BAND9756). On the evening before each flight (when birds were not present on the lek), ground control point (GCP) targets were placed across the lek in an

evenly spaced grid pattern and a survey-grade GPS was used to record the geographic location of each target. This provided geographic control to process imagery into an orthoimage and to estimate individual sage-grouse locations. Using similar methodologies as Hartmann et al. (2012), GCPs were manufactured using a polished aluminum surface with black duct tape to represent numbers used to identify each GCP (Figure 9).

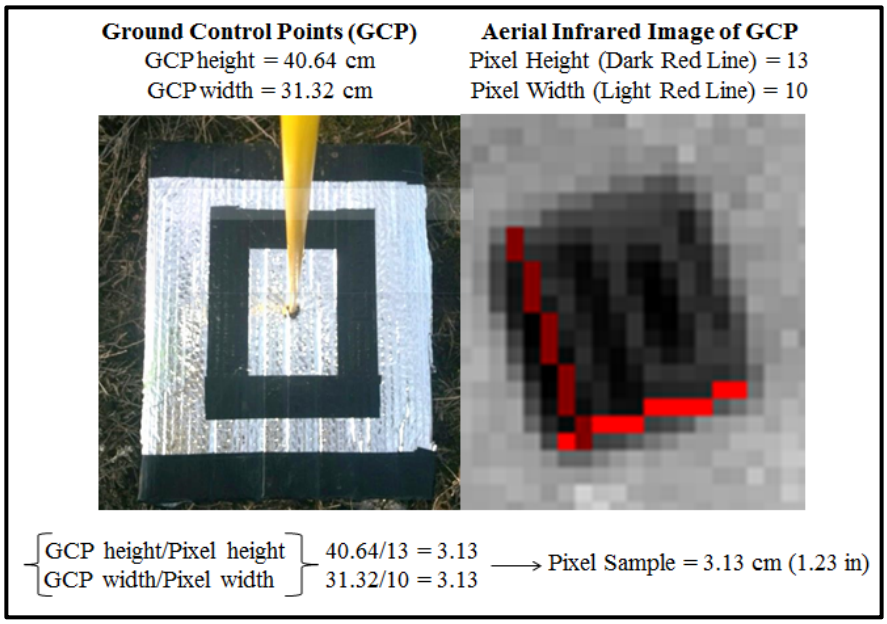

Figure 9. Ground control point (GCPs) used to geo-reference thermal imagery and sage grouse locations. The known GCP dimensions (i.e. height, width, and area) were also utilized to ground truth the anatomical dimensions of sage-grouse (length and area)

By utilizing materials with highly contrasting emissivity and reflectivity, such as polished aluminum (emissivity = 0.12, reflectivity = 88%) and black duct tape (emissivity = .92, reflectivity = .08), GCP targets were easily identified on the thermal and visible light imagery. The dimensions for each GCP were 40.64 cm (~16 in) x 31.32 cm (~12 in). Geographic coordinates of the center of each GCP were recorded using an

Ashtech ProMark 200 survey grade GPS receiver, manufactured by Coastal Instrument & Supply Company ©. This receiver utilizes the Utah Reference Network using a cellular link and has a positional accuracy of one centimeter. Ground control points were used to estimate pixel size, as well as to georeference imagery, and to determine locations of sage-grouse from the TIR imagery.

On the morning of each flight, before sunrise, a three-person flight crew consisting of the pilot, a secondary observer to identify other airborne objects (raptors, other planes, etc.), and a sage-grouse observer to record any behavioral reactions due to the RPA and to perform a traditional round count of sage-grouse before and after the aerial infrared survey arrived at the RPA launch site. The site chosen to launch the RPA was approximately 200 meters from the edge of the lek, behind a small building that

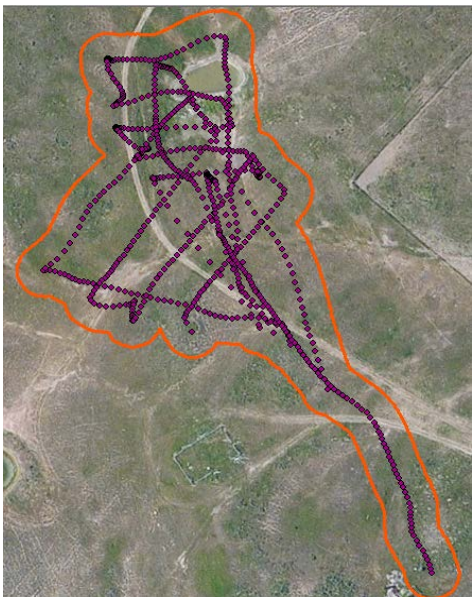

Figure 10. Nominal flight path for all 6 RPA flights. The purple points represent the global positioning system (GPS) data collected onboard the remotely piloted aircraft (RPA), in which the position data was captured every two seconds as the aircraft moved forward. Area inside the orange polygon represents the area within the field of view of the thermal sensor onboard the RPA.

acted as a blind. Before each flight, the RPA and imaging system underwent a pre-flight check to verify the flight plan, to evaluate the air-worthiness of the RPA, and to test the thermal camera.

The DJI S1000+ is a semi-autonomous system designed with an autopilot which receives instructions via a radio signal from a laptop running the autopilot software. A pre-determined flight plan is downloaded to the S1000+ which then launches, navigates to predetermined waypoints defining the flight path at a predetermined altitude and speed, returns to its home point once all waypoints have been reached and lands automatically (Figure 10). The same flight plan was used for all flights and varied only in altitude to test how the birds would react to the RPA.

All flights occurred at sunrise to comply with Federal Aviation Administration (FAA) regulations. To determine flight altitude and therefore image spatial resolution, a balance between vertical distance to sage-grouse (flying at lower altitudes would increase the potential to disturb the lek activity and flush the birds) and required image resolution to properly identify the birds needed to be met. When image spatial resolution is the only criteria, the selected altitude above ground level is determined by using simple geometry and the technical parameters of the sensor. These technical parameters included the horizontal and vertical fields of view and the resolution of the sensor. Figure 11 shows the general relationship between flight altitude, lens view angles and sensor resolution.

The FLIR A65sc used for this study was equipped with a 25mm lens with a horizontal field of view (HFOV) of 25˚, and a vertical field of view (VFOV) of 20˚. The 640 x 512 pixel matrix of the A65sc sensor means that the 640 pixels in the horizontal

dimension are distributed across the horizontal field of view of the lens. As the distance to the target increases, the field of view increases as a function of the tangent of ½ of the HFOV and the 640 pixels must therefore be distributed across a larger distance.

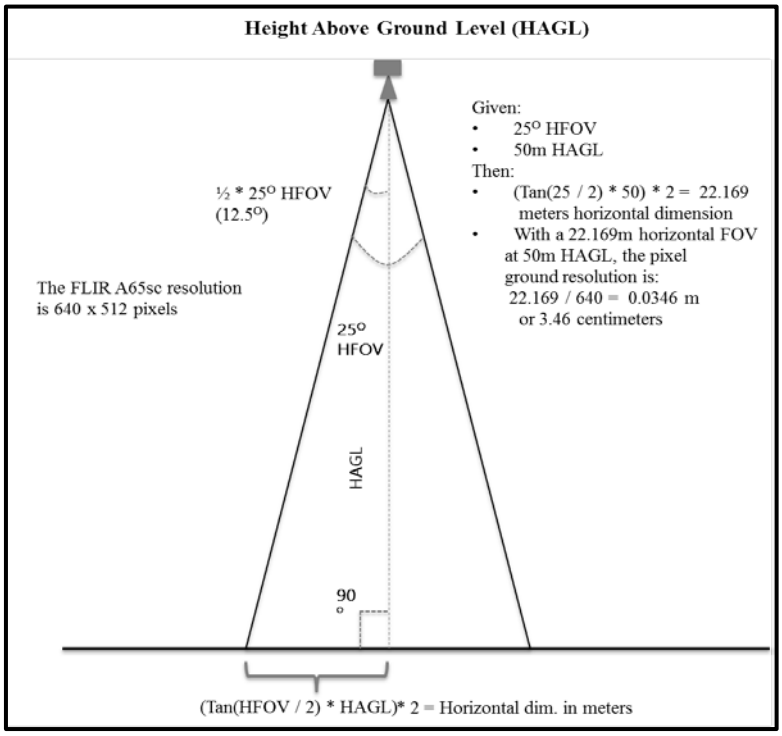

Figure 11. Diagrammatic relationship between distance to target, sensor view angle, resolution, and the resulting nominal pixel size

Data preparation

At the end of each flight, the thermal infrared video was downloaded and stored onto a portable 1TB hard disk, manufactured by Seagate Technology PLC (Public Limited Company). The thermal imagery was processed using the FLIR ResearchIR software (produced by FLIR Systems) to convert radiance values as collected by the camera to surface temperature values in °C. Individual frames of the processed video were exported to comma separated value (CSV) files. Each CSV file contained metadata

describing date, time, units of measure (Celsius), and frame number. The main body of the CSV files consisted of 640 columns and 512 rows representing the temperature measurements for each individual cell (pixel). CSV files were converted to non-compressed JPG files and each file linked to GPS derived Universal Transverse Mercator (UTM) coordinates recorded by the RPA by matching time stamps between the GPS and individual frames. This resulted in geo-tagged thermal rasters which were used to determine the geographic locations of individual birds.

The orthomosaic produced by Pix4D mapper Pro was used as a base map to aid in the placement of sage-grouse locations represented as points in an ArcGIS™ shapefile. The point shapefile was attributed with the anatomical and thermographic characterizations extracted from the thermal imagery. Pix4D utilizes automated digital photogrammetric techniques to create spatially accurate orthomosaics. The input data

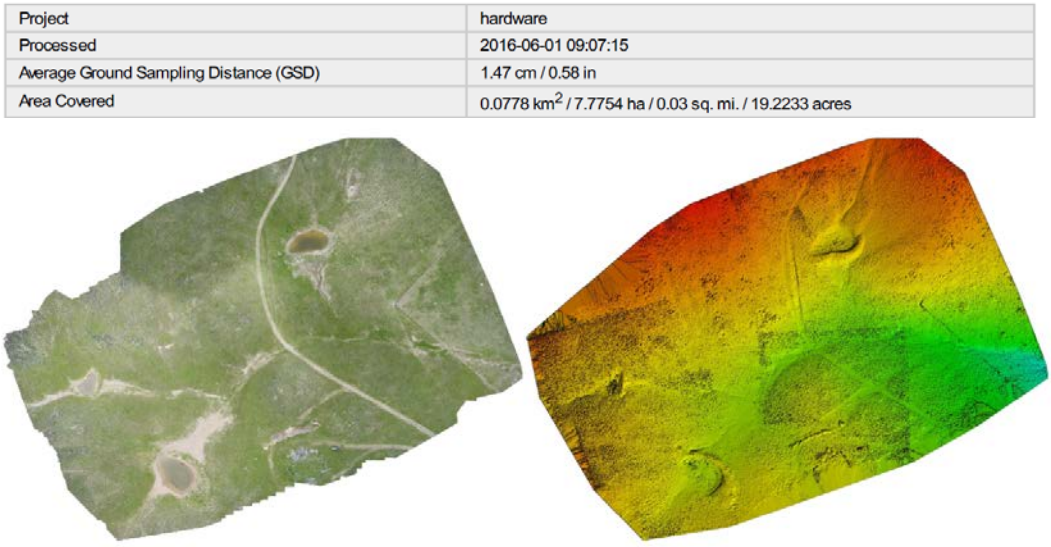

Figure 12. Orthomosaic and digital surface model (DSM) generated using Pix4D photogrammetric software. The auto generated orthomosaic and DSM were used as a ultra-high resolution basemap to aid in the sage-grouse mapping analysis process

required to generate the orthomosaic included the individual frames of geo-tagged digital aerial imagery along with the GPS surveyed locations of ground control points (GCP's). The Pix4D outputs from this nearly automated process include an orthomosaic and a digital surface model (DSM) (Figure 12).

Determining thermal difference between male and female sage-grouse

The initial identification of male and female sage-grouse from the thermal imagery utilized the same methodology as traditional ground observation. If a sage-grouse was observed displaying, it was classified as a male. We examined individual aerial infrared video frames and identified "displaying behavior" by observing the thermal flux of the forward portion of the bird as they displayed. The inflation and deflation of the apteria were easily detected due to the change in temperature as the birds strutted.

When no displaying behavior was observed we examined the length calculated from a pixel-based transect placed over the bird. Non-displaying males and females were identified based on length measured using a transect starting at the culmen and ending at the tail of each bird. If the sage-grouse had a transect length reflective of a male (66-67 cm length) or female (48-58 cm length) (Department of the Interior & Fish and Wildlife Service 2010) they were classified as such, using those metrics.

To calibrate the Stefan-Boltzman equation with the appropriate emissivity value to calculate temperatures for sage-grouse, an assumption was made that the emissivity of the apteria and eye combs are roughly similar to that of human skin. Human skin is estimated to have an emissivity of 0.98 (Buettner and Kern 1965). Therefore,

temperature calculations of all sage-grouse were estimated using an emissivity value of 0.98. Pixel values of the forward portion of displaying males (representing the apteria and eye combs) were sampled for multiple displaying males across all flights as well as the forward pixel values for females and non-displaying males.

Data analysis

Each identified bird was documented with a bounding region of interest (ROI) polygon representing the perimeter of the bird and its physical and thermal characteristics documented. The documented characteristics included the total length (transect line across the bird) total area as defined by a polygon representing the outline of the bird. Using the bird ROI, we extracted mean, maximum, minimum, and standard deviation temperature values.

After locating and characterizing sage-grouse individuals using the FLIR ResearchIR software, we then plotted their relative locations using ArcGIS™. Sage-grouse locations were manually digitized into an ArcGIS™ shapefile using the ultra-high resolution orthomosaic as a guide. Each of the 5 individual flights were digitized into different shapefiles. Only those birds identified and characterized with their respective thermal properties were placed into the shapefiles. In leveraging the digital archive, we examined the thermal video multiple times and mapped their spatial locations until no new sage-grouse individuals were being visually detected and monitored. Once a final GIS point layer was produced the process was conducted a second and third time to ensure the same number of sage-grouse we counted each time. Thus, every effort was made to visually detect, map, and identify every bird on the lek for each day. Figure 13

shows the flight path of the RPA and bird identifications from the thermal data.

Attributes for each bird location point consisting of thermal and physical characterizations of individual sage-grouse were entered into the feature class attribute table on a bird by bird basis. Sage-grouse individuals were documented and organized on a per flight basis to take the daily climate variability into consideration.

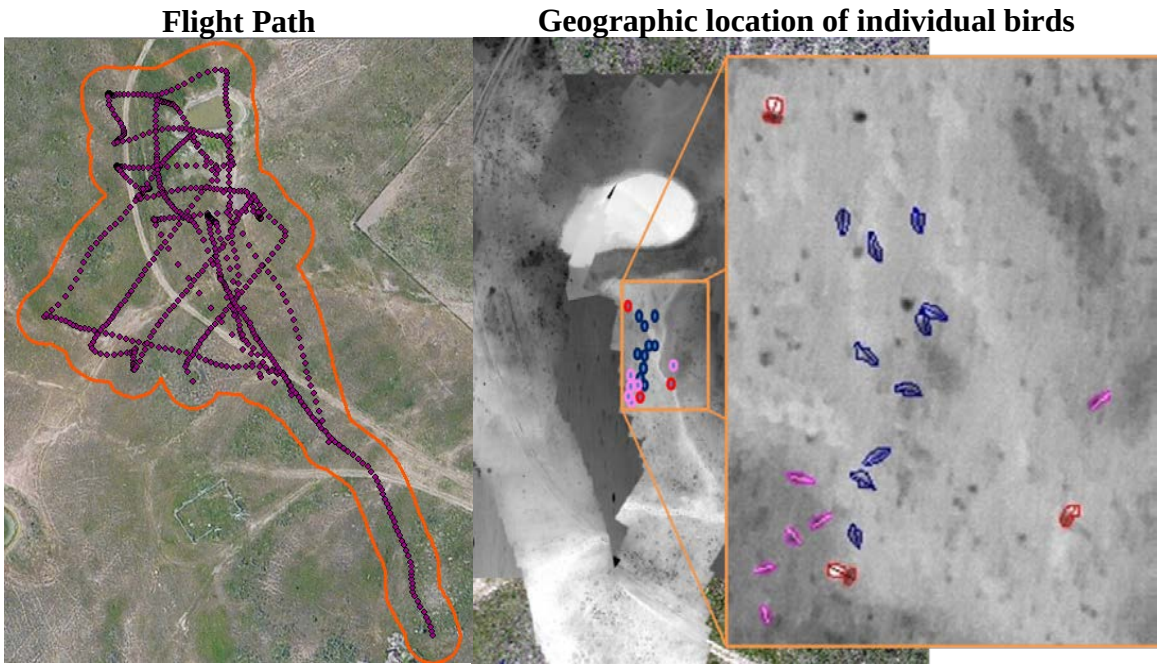

Figure 13. RPA flight path (left) and identified sage-grouse locations from thermal infrared images. Red birds represent displaying males, blue are non-displaying males, and pink are females.

Statistical analysis

The statistical analysis was focused on determining if there was a significant difference between thermal properties of sage-grouse due to sex and/or activity between males. We compared the thermal properties of identified females, non-displaying males, and displaying males using a Welch's t-test in R. The variables analyzed include the

minimum, maximum, mean, and range temperature values detected and archived originally in the spatial dataset. We tested the four different thermal data sets across all three sage-grouse classes. Due to the fact that we had a majority of males (67 non-displaying males and 22 displaying males) and far fewer females (28 females), a t-test that accounted for unequal variances and sample sizes was required.

The Welch's t-test is an adaptation of the Students t-test, in that it is more reliable when two samples have unequal variances and unequal sample sizes (Ruxton 2006). The null hypothesis is that the three sage-grouse classes have equal means. This is an independent sample t-test, commonly referred to as an unpaired test because they are typically applied to statistical units where two samples being compared do not overlap, where $\bar{X}$ is the sample mean, s^2 is the sample variance and N is the sample size for each population. In the Welchs t test the denominator is not based on a pooled variance estimate which is where this t-test differs from the Students t test.

$$t = \frac{\bar{X}_1 - \bar{X}_2}{\sqrt{\frac{s_1^2}{N_1} + \frac{s_2^2}{N_2}}}$$

The degrees of freedom accompanying the Welch's t test is associated with variance estimates, which is approximated using the Welch-Satterthwaite equation.

$$v \cong \frac{(\frac{s_1^2}{N_1} + \frac{s_2^2}{N_2})^2}{\frac{s_1^4}{N_1^2 v_1} + \frac{s_2^4}{N_2^2 v_1}}$$

The first variance estimate being $v_1 = N_1 - 1$ and the second variance estimate is$v_2 = N_2 - 1$. The Welch t-test makes the assumption that the two populations have normal distributions.

RESULTS

Geospatial data

We conducted six flights over a six-week period. Five of which were the aerial thermal infrared surveys using the FLIR A65sc conducted between March 5 –April 5, 2016. The final flight was conducted using the Sony A7r resulting in a series of still-frame digital aerial images used to generate the natural color orthomosaic. Combining all 5 individual flights we identified a total of 117 birds, or 23.4 birds per flight. On a per-flight basis we identified an average of 4.4 displaying males (22 / 5 flights), 13.4 non-displaying males (67 / 5 flights) (based on length and lack of displaying behavior observed on the thermal video collected by the RPA), and 5.6 females (28 / 5 flights) (based on size and length). We found that displaying males have a higher maximum temperature (27.52˚ C) and a wider temperature range (15.04 ˚ C) when compared to non-displaying males and females. Non-displaying males had an average maximum temperature of 17.24 ˚ C with a range of 4.6˚ C, and female sage-grouse had an average maximum temperature of 14.55 ˚ C with a range of 2.78 ˚ C.

Climate data was captured from the Utah Climate Center at Utah State University which collected data from the Hardware Ranch weather station (Table 1). Climate data for the dates and times (0600-0700 MST) of each overflight provide a means to calibrate the estimated bird temperatures to ambient conditions. The FLIR ResearchIR software calibrates and standardizes temperature values in rasterized data by setting the “Object Parameters” used for raster analysis with scientific accuracy. These settings can use known values of an object such as emissivity, distance to object, reflected temp, as well

Table 1. Average, hourly climate data collected by the Utah Climate Center from the Hardware Ranch weather station for the days and times (0600-0700 MST) for each overflight.

Flight	Air Temp (C˚)	Ground Temp (C˚)	Relative Humidity (%)	Solar Average (MJ)	Dew Point (C˚)	Above Ground Flight Alt. (m)
1	4.5	0	38.95	2.5	-10	40
2	9.7	0.28	60.96	0.89	1.9	50
3	11.67	2.39	39.24	2.8	-3.05	50
4	4.5	3.6	38.35	2.439	-11.56	45
5	15.22	3.11	19.76	3.15	-10.39	45

as the atmospheric conditions such as air temp and relative humidity. By defining these settings in FLIR ResearchIR the original data is overridden and calibrated using an algorithm based on Planck's Function. Our results used the known parameters to reduce any impacts of atmospheric affects had on the pixel values. Our results included the emissivity value set to 0.98, atmospheric conditions at time of aerial census, and distance to object as input parameters. This enabled us to calibrate our pixel sample data and accurately measure the theoretical radiance of sage-grouse across different days.

Sage-grouse lek displays are more active in the morning and this determined our target flight times between 0600 and 0700 MST. This time of day also improved our ability to separate individual birds from the soil and vegetation background. The morning flights coincided with the solar minimum which represents the point in time where the soil and vegetation background would be at its coldest temperature for the day. The relatively warmer birds against the contrasting cooler background made the identification easier.

Table 2. Spreadsheet calculating increasing spatial resolutions of thermal rasters for the thermal camera (FLIR A65sc) used in this study. Given the height above ground (HAGL), lens field of view (FOV), and sensor resolution, the pixel sample sizes can be estimated as the remotely piloted aircraft (RPA) increases height above ground level (HAGL).

Height AGL (m)	FOV (m)		Area (m^2)	X Resolution (cm)	Y Resolution (cm)
	Horizontal	Vertical			
10	4.434	3.527	16	0.69	0.69
20	8.868	7.053	63	1.39	1.38
30	13.302	10.580	141	2.08	2.07
40	17.736	14.106	250	2.77	2.76
50	22.169	17.633	391	3.46	3.44
60	26.603	21.159	563	4.16	4.13
70	31.037	24.686	766	4.85	4.82
80	35.471	28.212	1,001	5.54	5.51
90	39.905	31.739	1,267	6.24	6.20
100	44.339	35.265	1,564	6.93	6.89

Knowing the relationship between the height above ground level and the camera specifications (as seen in Figure 11), a spreadsheet that calculated image resolution was generated for different flight altitudes above ground level (Table 2). Our primary objective was to determine if we could identify individual birds and their thermal properties, we opted for flights that were 40 and 50m above ground level to minimize disturbance to bird activity. Pixel size was validated using the ground control points as reference.

Behavioral reactions to remotely piloted aircraft (RPA)

The sage-grouse response to the RPA was documented by the ground observer who counted the number of birds before each flight, and noted the total number of remaining birds on the lek immediately post flight. During the first flight conducted on

March 5th, 2016 (Flight 1) the ambient temperature was 4.5˚ C, the RPA height above ground was set at 40m, we had a preflight count of 13 sage-grouse individuals. As the RPA was launched from its home point location and as it approached the first waypoint in the flight path, the observer documented that the sage-grouse males had stopped displaying. When the RPA began its first banking maneuver by adjusting individual motor throttle, the sage-grouse flushed with five previously displaying males remaining, but hunched down in a protective stance. The sage-grouse may have flushed due to the RPAs height above ground level (HAGL), which we adjusted by increasing the HAGL to 50m for the second flight.

On our March 12th, 2016 aerial thermal infrared survey (Flight 2), the ambient temperature was 9.7˚ C the adjusted 50 m HAGL resulted in no sage-grouse flushing the lek. While the ground observer documented the same number of sage-grouse for both pre and post flight, we were unable to detect thermal responses representative of displaying male sage-grouse. The ground observer witnessed male sage-grouse displaying during the flight, however the thermal data did not yield a thermal responses indicative of displaying males, indicating that they had taken a protective stance.

The thermal infrared survey conducted on March 26th, 2016 (Flight 3), the ambient temperature was 11.7˚ C and was also flown at 50 m AGL and it was during this flight we detected the highest number of individual sage-grouse observations. Flight 3 was the first flight we were able to document the unique radiometric response produced by the apteria of adult male sage-grouse, which produces thermal responses that can be used to distinguish between male and female sage-grouse.

Our thermal infrared survey on April 2nd, 2016 (Flight 4) the ambient temperature was 4.5˚ C, but this flight was conducted at 45m AGL and resulted in our second highest count. In lowering our flight altitude to 45m we found that none of the sage-grouse flushed and continued their displaying behavior during the aerial survey, which may be indicative of familiarity. On this flight we also observed the highest number of displaying males. On April 5th, 2016 (Flight 5) the ambient temperature was 15.2˚ C , again we flew at 45m AGL and had similar findings as Flights 3 and 4. Because sage-grouse reaction to the RPA was based on observations with only 5 samples, we could not determine a specific reason that the birds flushed on the first flight, but did not flush on subsequent flights.

Ground census vs. areal census results

The number of sage-grouse for both the traditional ground counts and the aerial counts are compared in Figure 14 for each day of the study and were conducted simultaneously. Ground counts for the first flight resulted in a higher number of birds when compared to the aerial count. The aerial thermal infrared census conducted on March 12, 2016 resulted in a slightly higher thermal count compared to the ground count, but while the sage-grouse did not flush, we did not observe any displaying male sage-grouse on the thermal imagery. The first time we were able to capture thermal video containing displaying male sage-grouse was on the third (March 26th) flight which coincided with our highest count of sage-grouse and the most amount of displaying males (nine sage-grouse). This was also the flight where we had the largest degree of separation between the ground count and the aerial count. The April 2nd flight had a

higher count from the thermal imagery compared to the ground count, but the numbers were much more reflective of each other. On the April 5th flight, we were accompanied by the Hardware Ranch Manger who conducted an official lek census that has been documented with the Utah Division of Wildlife Resources (UDWR). The difference between the aerial count and the ground count from this final flight may have been due to two individual sage-grouse near the water feature on the southwest side of the lek, falling outside of the predetermined flight path, hence the RPA never passed over these individuals.

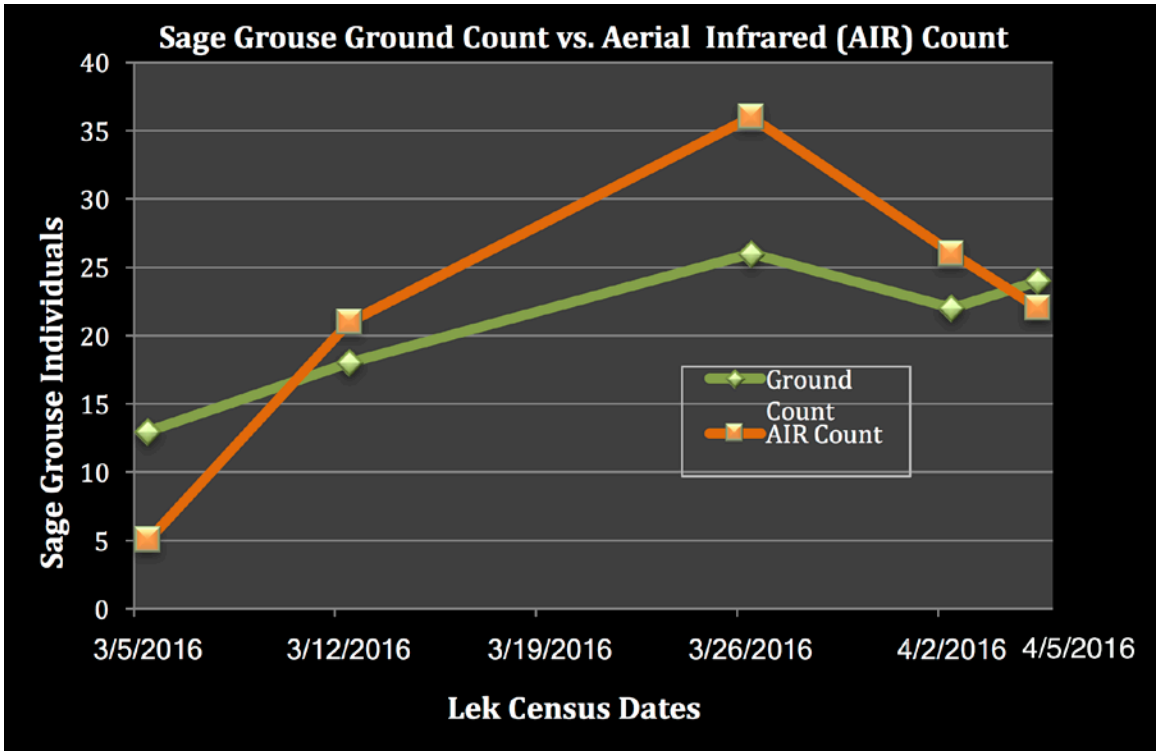

Figure 14. Comparison between the ground counts and aerial thermal infrared counts. Sage-grouse ground counts were done just minutes before starting the motors on the remotely piloted aircraft (RPA) to conduct the aerial census. The x axis shows the dates of each count and the y axis shows the total number of individual sage-grouse observed

Thermal differences between birds

Figure 15 plots individual birds identified from each flight and classified into the three categories based on size and display activity against the min and max temperature range per bird sampled on a given flight. Displaying males have typically the highest temperature readings (as expected) followed by non-displaying males (identified by size) and then females. Figure 15 indicated a relatively clean separation between the three categories with a few exceptions. The most significant exception is a non-displaying male in Flight 4 that fit the size characteristic of a male bird, but whose temperature range was below all other female birds. Inspection of the thermal image used to identify this bird showed odd anomalies with the pixel values and depicting a more "blurred" image compared to the others. Therefore, it is unknown if this bird was first misclassified (based on published length and size) as a non-displaying male (large female) or if the temperature measurements were biased in some way. There are also instances of a bird classified as a female based on length and size, but exhibiting temperature values more indicative of a non-displaying male. This may have been an immature male or a warmer female.

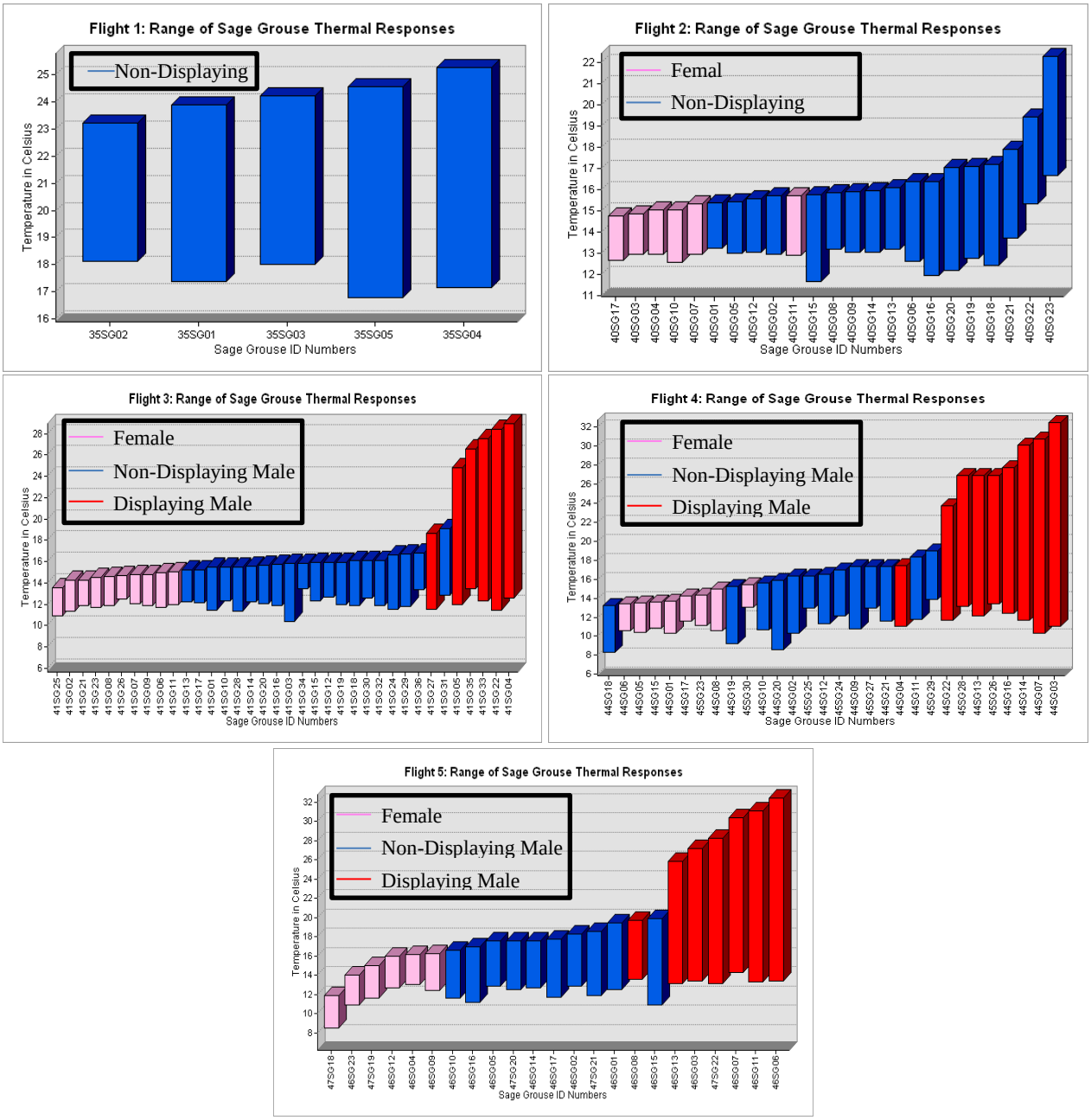

Figure 15. Comparison of thermal properties of birds classified as displaying males, non-displaying males, and females for each flight. Birds were classified based on size characteristics and whether they were displaying.

Characterizing thermal responses of sage-grouse

Daily climate variability (Table 1) was recorded to account for air temp and relative humidity when calculating the thermal response of individual sage-grouse. Atmospheric characteristics tend to affect the thermal response measured by the sensor due to its absorption and emission of thermal infrared radiation (Kaplan 1952). These environmental variables (air temperature, relative humidity (RH), solar input, and distance between the surface target and the infrared camera) affect the sensor and result in a lower surface temperature reading. Radiance measured at the sensor is a representation of the effective heat radiated by an object as well as the energy absorbed and/or emitted by the intervening atmospheric column between the target and the sensor. If the air temperature is less than that of the target, the atmosphere will absorb some of the radiant energy of the target resulting in a lower temperature reading. Conversely, if the air temperature is warmer than the target, the measurement at the sensor will appear warmer than it actually is. These errors introduced by atmospheric interference need to be taken into consideration when calculating target temperature.

The length and size (length and area of pixels) of sage-grouse aided in an initial determination of male vs. female sage-grouse, however the thermographic response for individual birds also provided a direct means of separation. As expected, the temperature of male sage-grouse was distinct due to their less insulated eyebrow patches and exposure of the apteria during displaying events. We used FLIR ResearchIR to examine the thermal response of displaying males, non-displaying males, and females. The region of interest (ROI) polygon and transect line described in the methods section was used to

sample both the total pixel area of individual sage-grouse as well as to extract the aggregate pixel mean, standard deviation, maximum, and minimum temperature values of each bird. The transect was used to examine the longitudinal thermal profile. Transect lines start at the sage-grouse's culmen and ran along the back of the sage-grouse ending at the tail. Figure 16 shows the ROI polygons and transects for 19 individual birds observed for Flight 3.

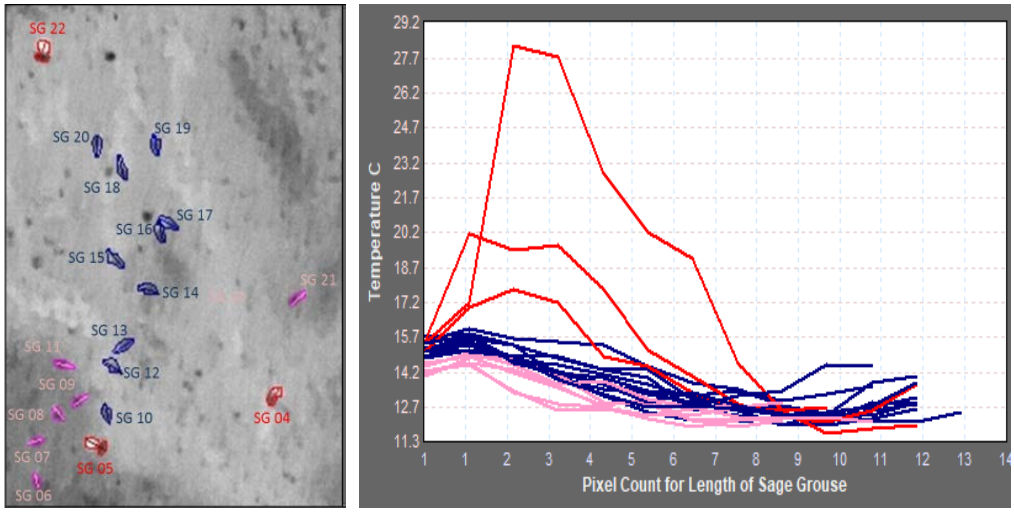

Figure 16. Thermal response of Displaying Males, Non-Displaying Males and Females for Flight 3. The response graph plots maximum temperature for each pixel along the line transect with the initial pixel representing the culmen.

Displaying males had a distinct temperature peak at the second and third pixel (approximate location of the apteria) and female transects were shorter by approximately 2 pixels with only a slight peak at the second pixel. Thermographic responses of individual sage-grouse for every flight can be found in Appendix A.

Table 3 shows the results from all five thermal infrared flights. Pixel resolution for each flight was estimated from Table 2 and refined by comparing the number of pixels falling across the photo targets against the known target size. Thus, flights 2 and 3, while flown at the same nominal altitude, had slightly different pixel resolutions.

Table 3. Summary of sage-grouse count results from 5 thermal census flights in Northern Utah. Flight Data is organized by date the flight took place and the height above ground (HAGL) level it was flown at. Estimated pixel sample size is also shown, which was used to detect and monitor thermal measurements of sage-grouse

Flight	Date	AGL Meters	Pixel size cm	Females	Males	Total Sage-grouse
1	3/05/2016	40	3 (1.18 in)	0	5	5
2	3/12/2016	50	3.68 (1.45 in)	6	17	23
3	3/26/2016	50	4.06 (1.6 in)	10	26	36
4	4/02/2016	45	3.12 (1.23 in)	7	23	30
5	4/05/2016	45	3.12 (1.23 in)	5	18	23

The displaying male, non-displaying male, and female temperature and size means for all sampled birds are found in Table 4. All birds had approximately equal minimum temperatures, but different maximum and mean temperatures with displaying males showing the highest max and mean temperatures. These differences are reflected in the temperature range. Bird area and length varied with non-displaying birds being longer than displaying males and females. We assume that the difference in area and length between displaying and non-displaying males is a function of the “posture” of the displaying male as he stands more erect and pushes out the chest and expands the wings in comparison.

Table 4. Summary of temperature and size data for the three sage-grouse categories (females, non-displaying males, and displaying Males). The thermal information collected for each class is maximum, mean, minimum and range in Celsius (C˚) and averaged. The averages for estimated length (cm) and area ($\mathbf{cm^2}$) have also been calculated

Category	Max. (C˚)	Mean (C˚)	Min. (C˚)	Range (C˚)	Length (cm)	Area (cm^2)	Sample Size
Females	14.55	12.97	11.77	2.79	37.11	324.99	28
Non-Displaying Males	17.23	14.38	12.57	4.66	46.94	487.90	67
Displaying Males	27.52	16.44	12.48	12.39	41.90	655.36	22
						Total	117

Mean maximum temperature of displaying males were approximately 10º C warmer than non-displaying males and 13 º C warmer than females. Maximum temperature affected mean temperature with displaying males approximately 2 º C warmer than non-displaying males which were 3.5 º C warmer than females. The wide range in maximum temperature between the bird classes is also reflected in the temperature range between classes. The temperature range for displaying males was 12.4 º C. Non-displaying males had a 4.6 º C temperature range and females ranged 2.8 º C between maximum and minimum temperatures. While displaying males were relatively easy to identify and separate from others using only temperature, non-displaying males and females proved to be more difficult to separate using thermal responses alone. Therefore, thermal responses coupled with bird length were the necessary metrics used separate non-displaying males from females. Figure 17 shows the geospatial location of each bird identified from the five thermal infrared surveys by class, as well as the locations of birds by individual flight.

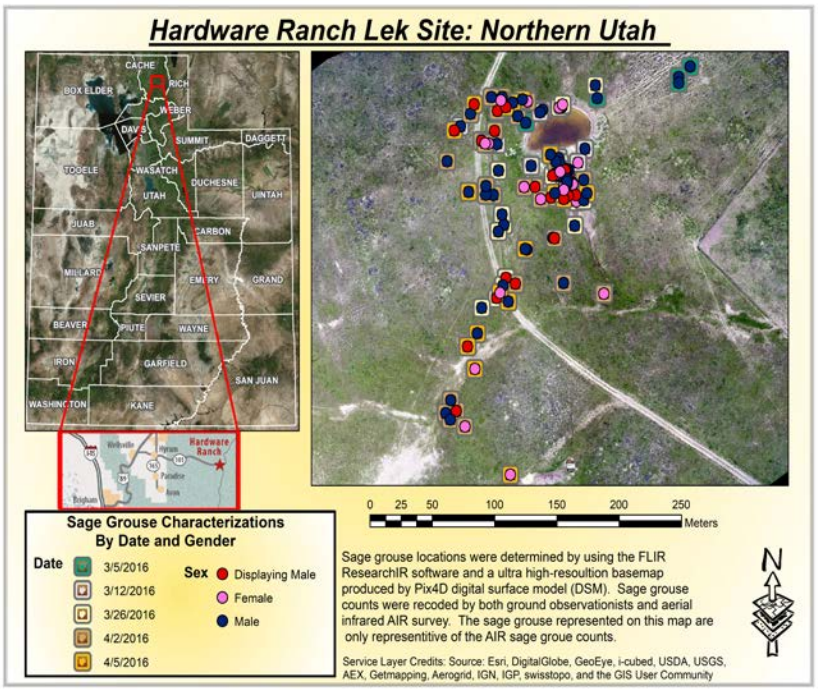

Figure 17. Spatial location of sage-grouse identified from 5 different flights spanning May 5th – April 5th, 2016.

Statistical analysis of thermal responses

Figure 18 displays boxplots of temperature and size characteristics for the three categories of sage-grouse. Boxplots display the median, quartiles, minimum, and maximum values for each category as well as outliers. The outliers were identified as bird related pixels collected at the edge of the lek during a turn of the RPA resulting in blurred images. From these plots, it's evident that displaying males showed different thermal and physical characteristics when compared to the non-displaying males and females. It was more difficult to determine if there were thermal differences between non-displaying male sage-grouse when compared to the female sage-grouse class. To determine if these differences were statistically significant, we used a Welch's T-test to

compare means and variances of thermal characteristics between the three bird classifications.

The results of the Welch Two Sample t-test can be seen in Table 5. Females and non-displaying males were the only two categories analyzed since displaying males showed such a clear contrast with the other two categories.

Table 5. Welch Two Sample t-test used to determine if maximum (max.), range, mean, and minimum (min.) temperature data is statistically significantly different between sage-grouse classes. The 3 sage-grouse classes were all tested but only the non-displaying male and female classes are displayed in this figure.

Parameter 1	Parameter 2	T statistic	p-value	95% CI	DF
Non-Disp. Male max.	Female max.	7.8433	<0.0001	2.009-3.372	91.892
Non-Disp. Male range	Female range	9.5157	<0.0001	1.487-2.272	86.124
Non-Disp. Male mean	Female mean	3.797	0.0002	0.672-2.148	91.129
Non-Disp. Male min.	Female min.	2.6045	0.01086	0.189-1.414	84.88

We found the largest difference between non-displaying male and female sage-grouse were, maximum temperature ($t=7.8$, $p<0.0001$), and the range of temperature ($t=9.5$, $p<0.0001$). Mean temperature ($t=3.8$, $p=0.0002$) and minimum temperature ($t=2.6$, $p=0.01086$) differences were less significant. We determined that the range of temperature and the maximum temperature were the best thermal responses to use as indicators to separate non-displaying male and female sage-grouse.

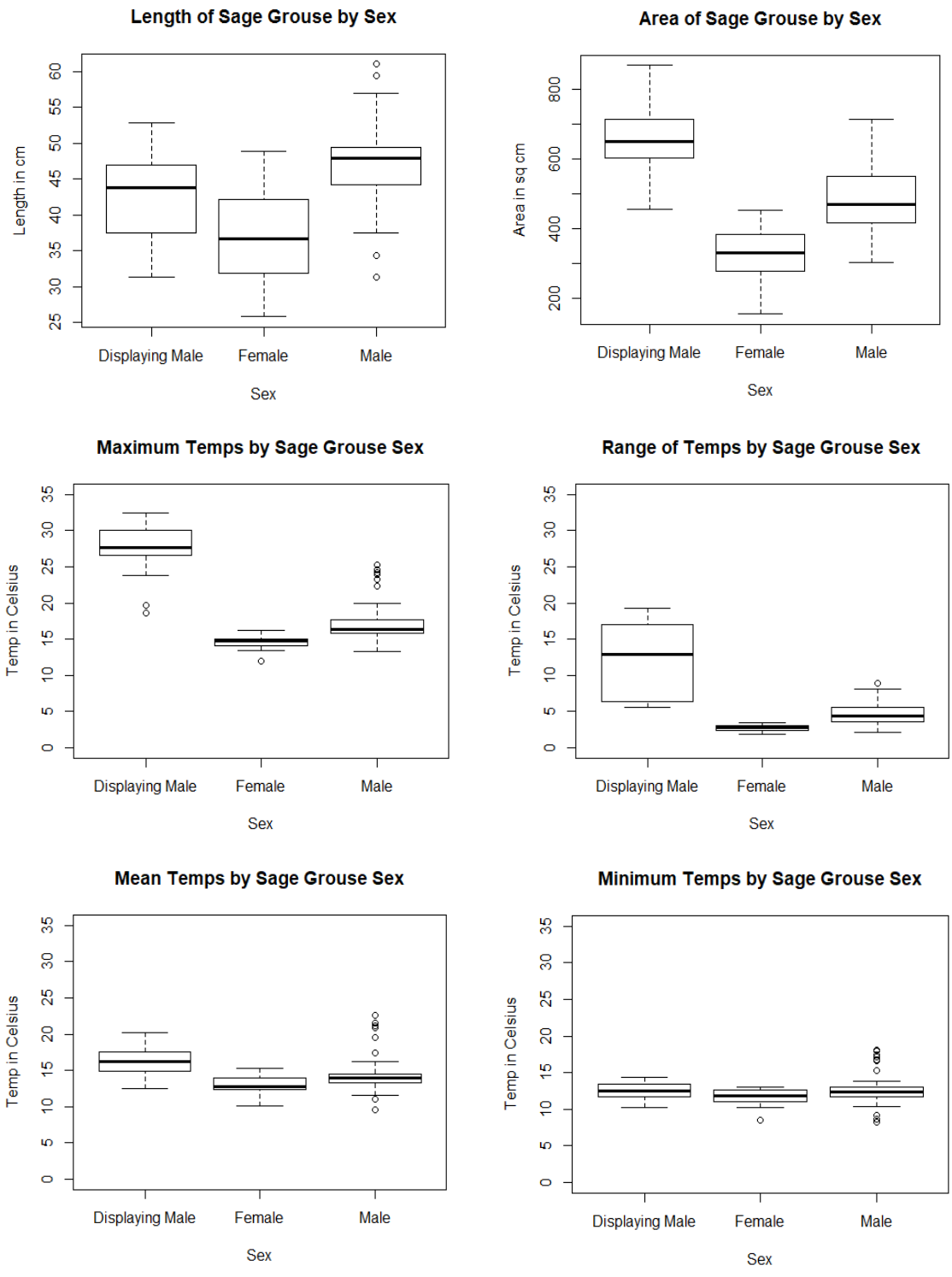

Figure 18. Boxplots of anatomical and thermal characteristics by sage-grouse classification

DISCUSSION

To better understand the responses of sage-grouse to RPA's, we reviewed the avian predation literature (Boyko et al. 2004, Dinkins et al. 2012, Hartzler 1974). Much of the literature on avian predation was more applicable to fixed wing aircraft (both manned and unmanned) as compared to multi-rotor, hovering aircraft. Gillette et al. (2013) used a Maule 7-235 fixed wing manned aerial platform and had flush occurrences when the aircraft was <150 m above ground level. In that same study a ground observer noted that the sage-grouse appeared to flush in response to the approaching aircraft. Vas et al. (2015) also evaluated the stress on birds when approached by an RPA, where they found that over 204 flights with a quadcopter that 80% of the time, birds were unaffected until within 4 meters. Scobie and Hugenholtz (2016) focused on the auditory impacts of the noise generated by the RPA and how that affects wildlife and found that the height of the RPA directly affected behavioral responses of 3 game species and 2 species of predators.

Fixed wing aircraft have many advantages over vertical Take-Off and Landing (VTOL) aircraft, however the physical structure and shape of a VTOL is significantly different compared to a fixed wing aircraft where fixed wing aircraft have a silhouette similar to that of traditional avian predators. The flight performance of a multi-rotor RPA is also unlike any avian predator known to sage-grouse. These differences indicate that sage-grouse may respond differently to a VTOL in comparison to a fixed wing aircraft. While we did not compare VTOL to fixed wing drones, we did make observations as to how the birds on our lek behaved as the RPA made multiple

overpasses.

On our first aerial survey the reason why we saw such a large difference between aerial count and the ground count is due to the sage-grouse flushing before the RPA reached their location as we had a camera in a fixed position. The 5 birds that remained on the lek appeared to be displaying males that ceased strutting. We can only assume that either our increase in flight altitude reduced the apparent threat to birds, or that the sage-grouse had become acclimated to the presence of the RPA and no longer considered it a threat.

We have shown that sage-grouse can be detected and inventoried using thermal imagery collected during the early morning hours at sunrise when the thermal minimum has been reached. Measurements collected from the thermal infrared camera included maximum, minimum, and mean temperatures along with physical measurements of bird length and size (area from a vertical perspective). Where length is concerned, our measurements varied from what has been published in the literature. The length and area statistics were the result of the length of the transect and the area of the polygon drawn around each bird. We calculated size and length based on the number of pixels occupying either the polygon or transect, but in doing this we know there is some error. Pixel resolution was determined by comparing the number of pixels spanning our ground control photo targets to the actual size of the target. The size of sage-grouse measured in this way varied from the measurements reported by the Department of the Interior & Fish and Wildlife Service (2010). Their findings showed that adult males were roughly 66 cm in length, and females were approximately 48 cm in length. Our findings showed that

non-displaying males were, on average, 47 cm in length and female sage-grouse were, on average, 37 cm in length. Our measurements are relatively conservative in comparison which may be due to using raster based thermal images rather than physically measuring the sage-grouse. This shows that the measurements may differ due to using average pixels, posture of the bird, or the edges of the bird blend into the ground cover making the pixel samples found in the transect and polygon were consistently conservatively drawn.

We validated bird sex by looking at behavior with birds surrounding displaying males as females and birds outside of those clusters and those that were chased by displaying males as other males. The reason for our observed shorter length measurements could be many-fold, when the ROI lines were drawn to sample the sage-grouse individuals we purposefully underestimated the pixels being sampled to ensure that ground cover pixels were not being sampled, which would pollute the thermal measurements. The edges between features (transition between one feature and another) within an image are often graduated across 2-3 pixels making the identification of the true edge a challenge. By underestimating the pixels, we are sampling we can ensure that we are only sampling pixels that represent sage-grouse temperature values and this could have resulted in smaller length and area measurements. Another compounding factor is the deterioration of pixel accuracy due to the increasing pixel size. The larger the pixel the greater the uncertainty over a given area represented by pixels forming the transition between features. Another possible reason for the difference in measurements is that we did not capture and physically measure the birds. Not only is this a difference in

measurement techniques, but also, the thermal imagery captured the birds in a standing stance making their apparent longitudinal profile from a vertical point of view, shorter.

We found that the area measurement of sage-grouse individuals was the best anatomical metric used to identify the sex of the sage-grouse. While non-displaying males were longer than that of the displaying males, the area of the displaying males ($655cm^2$) was much larger than that of the non-displaying male ($488cm^2$). This difference was even more evident when comparing displaying males to female sage-grouse ($325cm^2$). We found that displaying males are roughly twice the size of female sage-grouse, which is consistent to literature. Remotely Piloted Aircraft are effective tool in measuring the anatomical and thermal characteristics of wildlife and may be less invasive. Sage-grouse areas are, therefore, an important metric in determining whether a sage-grouse is male or female from aerial imagery. Using sage-grouse area as an indicator of sage-grouse sex using remotely sensed data, to our knowledge, has never been used. Sage-grouse areas are something, we believe, should be leveraged in classifying sage-grouse sex. With area measurements, it is possible to use object oriented classification tools such as E-Cognition™ to automate a process that utilizes feature shape, length, and thermal characteristics to detect and characterize sage-grouse using thermal imagery.

We also found that birds observed at the edge of frames when the RPA was conducting a banking maneuver tended to become blurry and produced temperature results that contradicted the area and size measurements. In short, birds that were characterized as non-displaying males based on size also showed temperature

measurements characteristic of females. We would typically eliminate such individuals, except that they did indeed constitute a count and since they were located at the extreme edge of our flight area, these observations were not repeated when the RPA settled into its normal flight attitude so that we could get a better reading. In future work I would suggest that a 10-20m buffer should be added to a flight area to try to capture the immediate area surrounding a lek. This could aid in detecting sage-grouse on the far reaches of the lek perimeter or predators surrounding a lek

The use of an RPA to collect imagery that can detect sage-grouse provides an opportunity to better inventory leks in areas that are difficult to reach. A point feature database extracted from this imagery of sage-grouse lek activity provides opportunities for future analysis of bird spatial distributions as a function of social behavior

CONCLUSION

With RPAs becoming easier to fly and more economically accessible we will see them leveraged more and more in the scientific community. The software used to process and analyze imagery collected using RPAs is becoming more available and easy to use as well. These advances in the hardware and software surrounding RPAs will provide land managers with a powerful tool to aid in natural resource assessment, monitoring, and management. Many RPAs are already packaged with sophisticated autopilot systems that can be easily programmed fly along pre-determined paths. Photogrammetric software has been automated to the point that the user simply needs to input the set of individual digital photos collected by the RPA to produce a usable ortho-corrected base map complete with a topographic point cloud. Managers who require more rigor in their data output can contract with a number of companies who specialize in the processing of imagery (as well as collection) without an investment in software, equipment, or flight training.

In this study, we found that a multi-rotor platform fitted with thermal and visible spectrum cameras provided a viable means of inventorying sage-grouse lek attendance. The advantage of using RPAs to record wildlife activity as well as assess vegetation communities, is the ability to capture field conditions at the time of the overflight. By conducting an aerial survey of wildlife using videography you also collect data that allows scientists to evaluate interactions between individuals. While the RPA and camera is being used to study wildlife, the landscape features (water bodies, rock outcrops, roads, drainages, etc.), and land cover conditions are documented. Using this

technology makes it possible to collect more information regarding habitat environmental and conditions during the time the wildlife survey is conducted. Another advantage is that remotely sensed imagery collected by a thermal camera allows us to measure anatomical data of wildlife without having to come into physical contact. Multiple overflights across the same location, in our case a lek, provides a means to understand and document social interactions between individuals and how those interactions are repeated through time. In this study we were able to document the anatomical characteristics (size and temperature) of sage-grouse using imagery collected by a thermal camera and use those differences to categorize birds into three different classes defined by sex and display activity. While we determined that temperature could be used as an indicator of sage-grouse sex, others have explored the diet and level of activity of wildlife which also affects thermal characteristics. Moen (1968) stated:

> "The quantity of heat lost by the animal must be balanced against the heat produced by metabolic processes. Each of the major factors contributing to heat loss, including conduction, convection, radiation, and evaporation, must be considered as well as differences in the amount of heat produced by the animal on different diets and at different levels of activity. Thus the game manager is forced to distinguish between both the quantity and quality of food and cover on a range and their combined energetic effects on the physiological response of the animal."(Moen,1968).

As Moen (1968) found, thermal data could potentially be used to examine health of wildlife. Hurnik et al. (1984) suggested using thermal imaging on cattle to detect health disorders. Early detection of sickened wildlife (especially pack and herd animals) or individual cattle, can aid in mitigating disease outbreaks. Using thermal imaging systems to document and catalog the average emittance of thermal radiation by a healthy

animal can potentially lead to the use of these systems to identify thermal anomalies that may indicate animal health.

Using remotely sensed data to identify the spatial distribution of wildlife can give wildlife managers better insight to both intraspecific and interspecific relationships. The integration of animal locations within a Geographic Information System can be analyzed using spatial pattern analysis techniques such as Kernel Density Estimation (KDE). The KDE is a density function that tests for spatial randomness and provides a visualization of geographically distributed densities as an estimate of the number of events per unit area allowing managers to assess "hot" and "cold spots" on a map base. These hot and cold spots can guide managers to areas that are heavily utilized (or not) by livestock or wildlife and use that information to better understand animal behavior as well as habitat preferences.

Visual (qualitative) analysis of the thermal imagery showed that displaying males were easily identified due to the appearance and disappearance of the aptera as they strutted to attract females. However, it was difficult to visually separate non-displaying males from female sage-grouse due to their similar temperatures. However, using a Welch's T-test, we found that the thermal response for non-displaying males and females were statistically different with maximum temperature and temperature range being the most significantly different metrics. In comparison, other studies using RPA and thermal cameras mounted to fixed-wing aircraft were not able to differentiate sage-grouse by sex. Hanson et al. (2014) used a thermal camera and a standard RGB camera onboard a Raven RQ-11 (a fixed wing RPA) and were able to detect sage-grouse individuals but were

unable to identify sex. Gillette et al. (2015), using a Maule 7-235 fixed wing manned aerial platform and a Mid-wav infrared RS67000 gyro stabilized camera, were also unable to determine the sexual classifications of sage-grouse individuals. A primary difference in our technique is in the use of a rotary, hovering platform that allowed us to fly lower and slower and therefore collected imagery with finer resolution.

We found that the RPA overflights caused the female (and possibly non-displaying male) sage-grouse occupying the lek to flush only during the first flight when the RPA flew at 40m above ground level (AGL). Strutting males remained on the lek, but ceased their strutting activity and crouched into a defensive position. In comparison, a study using a traditional fixed wing manned aircraft observed sage-grouse flushing when flying at <150 AGL (Gillette et al. 2013). On our subsequent four flights, sage-grouse did not flush and on the third flight, strutting activity was not interrupted. We therefore found that using RPA to collect high resolution thermal imagery appears to be an effective and potentially less invasive census tool to document sage-grouse numbers and activity on leks.

To the best of our knowledge we are the first study to show that thermal responses of sage-grouse collected by a low-flying RPA can be used to differentiate between males and females. We have also demonstrated that this technique can document spatial distribution of individual sage-grouse allowing wildlife managers to better understand lek behavior. An additional benefit of this technique is the ability to develop a permanent digital archive of sage-grouse lek activity, environmental conditions, and landscape

characteristics that can be analyzed at different times and compared to other aerial surveys across space and time.

Using Remotely piloted aircraft for natural resource management and monitoring is growing tremendously (Stark et al. 2014). With the cost of RPA systems and cameras decreasing and their capability increasing, their use as research and management tools will become more commonplace (Rango et al. 2006). The FAA conservatively estimates 8,000 drones are flying in U.S. airspace, with as many as 30,000 by 2020 (Martin 2014). It seems an obvious conclusion that these instruments will become an important tool for natural resource managers in the future.

Our proof of concept study contributes to the body of research aimed at developing best practices in the use of drones for ecological research. This work also addresses calls for assessments of impacts to wildlife as a result of the use of these tools (Vas et al. 2015). While this technology has its limitations, such as range and flight duration (Watts et al. 2010), using state of the art technology to obtain accurate sage-grouse lek attendance counts can help managers and scientists better understand lek attendance and lek population dynamics. Further, results of this study will also provide a set of guidelines for the use of RPA's to monitor sage-grouse.

The use of high resolution (1-4cm) airborne imagery to census wildlife – in this case sage-grouse, can lead to a better understanding of animal behavior characteristics as well as their spatial distribution (Gillette et al. 2015). In addition, high-resolution imagery coupled with extracted 3-D point clouds that characterize surface (including vegetation) topography provide an enhanced ability to characterize the physical

characteristics and distribution of vegetation components (i.e. shrub density, cover, height, etc.) in and around leks. While this effort is focused on the detection and census of sage-grouse, the technology and resulting data can enhance research efforts in a variety of ecological and land management disciplines (Hanson et al. 2014, Martin 2014, Rango et al. 2006, Rango et al. 2009).

LITERATURE CITED

Blevin, W. R., and W. J. Brown. 1971. A Precise Measurement of the Stefan-Boltzmann Constant. Metrologia 7:1–15.

Blomberg, E. J., J. S. Sedinger, D. V. Nonne, and M. T. Atamian. 2013. Annual male lek attendance influences count-based population indices of greater sage-grouse. The Journal of Wildlife Management 77:1583–1592.

Boyko, A. R., R. M. Gibson, and J. R. Lucas. 2004. How Predation Risk Affects the Temporal Dynamics of Avian Leks: Greater Sage Grouse versus Golden Eagles. The American Naturalist 163:154–165.

Buettner, K. J. K., and C. D. Kern. 1965. The determination of infrared emissivities of terrestrial surfaces. Journal of Geophysical Research, 70:1329–1337.

Casana, J., J. Kantner, A. Wiewel, and J. Cothren. 2017. Archaeological aerial thermography: a case study at the Chaco-era Blue J community, New Mexico. Journal of Archaeological Science 45:207–219.

Connelly, J. W., K. P. Reese, and M. Schroeder. 2003. Monitoring of Greater Sage-Grouse Habitats and Populations. College of Natural Resources Experiment Station Bulletin 80. University of Idaho, Moscow Idaho, USA.

Connelly, J. W., and M. A. Schroeder. 2007. Historical and current approaches to monitoring greater sage-grouse. Monitoring Populations of Sage-Grouse. College of Natural Resources Experiment Station Bulletin 88:3–9.

Dahlgren, D. K., M. R. Guttery, T. A. Messmer, D. Caudill, R. Dwayne Elmore, R. Chi, and D. N. Koons. 2016. Evaluating vital rate contributions to greater sage-grouse

population dynamics to inform conservation. Ecosphere 7:3

Department of the Interior, & Fish and Wildlife Service. 2010. Endangered and Threatened Wildlife and Plants; 12-Month Findings for Petitions to List the Greater SageGrouse (*Centrocercus urophasianus*) as Threatened or Endangered.

Department of the Interior, & Fish and Wildlife Service. 2015. Endangered and Threatened Wildlife and Plants; 12-Month Finding on a Petition To List Greater Sage-Grouse (*Centrocercus urophasianus)* as an Endangered or Threatened.

Dinkins, J. B., M. R. Conover, C. P. Kirol, and J. L. Beck. 2012. Greater Sage-Grouse (*Centrocercus urophasianus*) Select Nest Sites and Brood Sites Away from Avian Predators. The Auk 129:600–610.

Doherty, K. E., J. S. Evans, P. S. Coates, L. M. Juliusson, and B. C. Fedy. 2016. Importance of regional variation in conservation planning: a rangewide example of the Greater Sage-Grouse. Ecosphere 7:10.

Fremgen, A. L., C. P. Hansen, M. A. Rumble, R. S. Gamo, and J. J. Millspaugh 2016. Male greater sage-grouse detectability on leks. The Journal of Wildlife Management 80:266–274.

Gillette, G. L., P. S. Coates, S. Petersen, and J. P. Romero. 2013. Can Reliable Sage-Grouse Lek Counts Be Obtained Using Aerial Infrared Technology? Journal of Fish and Wildlife Management 4:386–394.

Gillette, G. L., K. P. Reese, J. W. Connelly, C. Colt, and J. M. Knetter. 2015. Evaluating the potential of aerial infrared as a lek count method for prairie grouse. Journal of Fish and Wildlife Management 6:486–497.

Guttery, M. R., T. A. Messmer, E. T. Thacker, N. Gruber, and C. M. Culumber. 2013. Greater sage-grouse sex ratios in Utah: Implications for reporting population trends. The Journal of Wildlife Management 77:1593–1597.

Hanson, L., C. L. Holmquist-Johnson, and M. L. Cowardin 2014. Evaluation of the Raven sUAS to detect and monitor greater sage-grouse leks within the Middle Park population (USGS Numbered Series No. 2014–1205) (p. 24). U.S. Geological Survey.

Hartmann, W., S. Tilch, H. Eisenbeiss, and K. Schindler. 2012. Determination of the UAV position by automatic processing of thermal images. ISPRS–Int. Arch. Photogramm, Remote Sensing. Spatial Information 39: B6.

Hartzler, J. E. 1974. Predation and the Daily Timing of Sage Grouse Leks. The Auk 91:532–536.

Hurnik, J. F., S. D. Boer, and A. B. Webster. 1984. Detection of Health Disorders in Dairy Cattle Utilizing a Thermal Infrared Scanning Technique. Canadian Journal of Animal Science 64:1071–1073.

Johnson, D. H., and M. M. Rowland . 2007. The utility of lek counts for monitoring greater sage-grouse. Monitoring Populations of Sage-Grouse. College of Natural Resources Experiment Station Bulletin 88:15–23.

Jones, G. P., L. G. Pearlstine, and H. F. Percival. 2006. An Assessment of Small Unmanned Aerial Vehicles for Wildlife Research. Wildlife Society Bulletin 34:750–758.

Kaplan, L. D. 1952. On the calculation of atmospheric transmission functions for the

infrared. Journal of Meteorology 9:139–144.

Knick, S. T., S. E. Hanser, and K. L. Preston. 2013. Modeling ecological minimum requirements for distribution of greater sage-grouse leks: implications for population connectivity across their western range, U.S.A. Ecology and Evolution 3:1539–1551.

Martin, C. 2014. The Drone Debate: The Intersection of Drone Technology and Wildlife Work. The Wildlife Professional 8:18–23.

Moen, A. N. 1968. Surface Temperatures and Radiant Heat Loss from White-Tailed Deer. The Journal of Wildlife Management 32:338–344.

Opar, A. 2015. Tick Tock Goes the Sage-Grouse Conservation Clock. Audubon. Sept.-Oct.:1–3.

Rango, A., A. Laliberte, J. E. Herrick, C. Winters, K. Havstad, C. Steele, and D. Browning. 2009. Unmanned aerial vehicle-based remote sensing for rangeland assessment, monitoring, and management. Journal of Applied Remote Sensing 3:35–42.

Rango, A., A. Laliberte, C. Steele, J. E. Herrick, B. Bestelmeyer, T. Schmugge, and V. Jenkins, 2006. Using Unmanned Aerial Vehicles for Rangelands: Current Applications and Future Potentials. Environmental Practice 8:159–168.

Rowland, M. M., M. J. Wisdom, L. H. Suring, and C. W. Meinke. 2006. Greater sage-grouse as an umbrella species for sagebrush-associated vertebrates. Biological Conservation 129:323–335.

Ruxton, G. D. 2006. The unequal variance t-test is an underused alternative to Student’s

t-test and the Mann–Whitney U test. Behavioral Ecology 17:688–690.

Scobie, C. A., and C. H. Hugenholtz . 2016. Wildlife monitoring with unmanned aerial vehicles: Quantifying distance to auditory detection. Wildlife Society Bulletin, 40:781–785.

SoilWeb: An Online Soil Survey Browser, California Soil Resource Lab. 2016. Retrieved February 21, 2017, from https://casoilresource.lawr.ucdavis.edu.

Stark, B., B. Smith, and Y. Chen 2014. Survey of thermal infrared remote sensing for Unmanned Aerial Systems. International Conference on Unmanned Aircraft Systems (ICUAS) 2014:1294–1299.

U.S. Department of Agriculture, Natural Resource Conservation Servic. 2012. Ecological Site Descriptions. Retrieved January 21, 2017, from https://esis.sc.egov.usda.gov

Vas, E., A. Lescroël, O. Duriez, G. Boguszewski, and D. Grémillet . 2015. Approaching birds with drones: first experiments and ethical guidelines. Biology Letters 11:1–2

Watts, A. C., J. H. Perry, S. E. Smith, M. A. Burgess, B. E. Wilkinson, Z. Szantoi, and H. F. Percival. 2010. Small Unmanned Aircraft Systems for Low-Altitude Aerial Surveys. Journal of Wildlife Management 74:1614–1619.

Western Regional Climate Center, Hardware Ranch Utah, Climate Summary. 2006. Retrieved February 26, 2017, from http://www.wrcc.dri.edu

APPENDIX

Table A-1. Sage-grouse individuals are separated by flight, where first sage-grouse observed during the flight was documented with the video record number and then the sage-grouse number. For instance, the first flight was documented using the video record number (35). Then the first sage-grouse observed in the video record was labeled SG01 and the last observed bird was labeled SG05 (naming convention example: 35SG01 - 35SG05). The thermal and anatomical characteristics were detected and archived on an individual sage-grouse level without ever having physical contact with the sampled specimen.

Flight	SG ID	Sex	Max. (C˚)	Mean T. in (C˚)	Min T. in (C˚)	Range (C˚)	Length (cm)	SG Area (cm^2)
1	35SG01	Male	23.89	20.83	17.39	6.50	50.95	540.52
1	35SG02	Male	23.22	20.89	18.11	5.11	47.96	540.52
1	35SG03	Male	24.22	21.17	18.00	6.22	41.96	525.29
1	35SG04	Male	25.28	22.56	17.17	8.11	53.95	525.29
1	35SG05	Male	24.56	21.50	16.78	7.78	47.96	525.29
2	40SG01	Male	15.39	14.17	13.22	2.17	44.20	467.74
2	40SG02	Male	15.72	14.11	12.94	2.78	47.88	495.81
2	40SG03	Female	14.83	14.28	12.94	1.89	36.83	383.55
2	40SG04	Female	15.06	14.28	12.94	2.11	40.51	364.84
2	40SG05	Male	15.44	14.28	13.00	2.44	44.20	420.97
2	40SG06	Male	16.39	14.28	12.61	3.78	47.88	533.22
2	40SG07	Female	15.33	14.00	12.94	2.39	29.46	308.71
2	40SG08	Male	15.83	14.11	13.17	2.67	44.20	420.97
2	40SG09	Male	15.89	14.22	13.06	2.83	40.51	355.48
2	40SG10	Female	15.06	14.44	12.56	2.50	25.78	271.29
2	40SG11	Female	15.72	14.33	12.89	2.83	29.46	290.00
2	40SG12	Male	15.56	14.17	13.06	2.50	47.88	561.29
2	40SG13	Male	16.11	14.67	13.17	2.94	44.20	439.68
2	40SG14	Male	15.94	14.50	13.06	2.89	40.51	439.68
2	40SG15	Male	15.78	13.44	11.67	4.11	44.20	392.90
2	40SG16	Male	16.39	14.06	11.94	4.44	40.51	402.26
2	40SG17	Female	14.78	13.50	12.67	2.11	25.78	280.64
2	40SG18	Male	17.17	14.67	12.44	4.72	51.56	449.03
2	40SG19	Male	17.11	14.78	12.78	4.33	44.20	392.90
2	40SG20	Male	17.06	15.22	12.17	4.89	44.20	402.26
2	40SG21	Male	17.89	16.11	13.72	4.17	47.88	439.68
2	40SG22	Male	19.44	17.44	15.33	4.11	47.88	411.61
2	40SG23	Male	22.28	19.61	16.67	5.61	40.51	420.97
3	41SG01	Male	15.50	13.00	11.44	4.06	52.83	474.84
3	41SG02	Female	14.23	12.61	11.34	2.89	44.70	330.32
3	41SG03	Male	15.83	12.22	10.39	5.44	56.90	516.13
3	41SG04	Disp.	28.94	14.33	12.56	5.56	40.64	454.19

		Male						
3	41SG05	Disp. Male	24.83	15.44	11.94	9.72	48.77	588.39
3	41SG06	Female	14.97	12.79	11.71	3.26	28.45	154.84
3	41SG07	Female	14.75	12.68	12.06	2.69	36.58	165.16
3	41SG08	Female	14.64	12.93	11.89	2.74	32.51	227.10
3	41SG09	Female	14.75	12.81	11.85	2.90	36.58	247.74
3	41SG10	Male	15.50	13.17	12.28	3.22	48.77	309.68
3	41SG11	Female	15.04	12.88	11.94	3.10	44.70	330.32
3	41SG12	Male	15.94	14.00	12.67	3.28	44.70	412.90
3	41SG13	Male	15.22	13.44	12.22	3.00	48.77	474.84
3	41SG14	Male	15.56	13.33	12.22	3.33	48.77	402.58
3	41SG15	Male	15.90	13.74	12.33	3.57	44.70	443.87
3	41SG16	Male	15.72	13.31	11.85	3.87	48.77	423.22
3	41SG17	Male	15.22	13.67	12.17	3.06	48.77	454.19
3	41SG18	Male	16.11	13.67	11.89	4.22	52.83	423.22
3	41SG19	Male	15.94	13.56	11.94	4.00	48.77	402.58
3	41SG20	Male	15.67	13.06	12.06	3.61	48.77	392.26
3	41SG21	Female	14.28	12.83	11.89	2.39	40.64	278.71
3	41SG22	Disp. Male	28.44	16.50	11.44	17.00	48.77	650.32
3	41SG23	Female	14.50	12.56	11.67	2.83	48.77	371.61
3	41SG24	Male	16.67	13.83	11.56	5.11	52.83	557.42
3	41SG25	Female	13.56	11.67	10.94	2.61	44.70	381.93
3	41SG26	Female	14.72	13.39	12.50	2.22	40.64	237.42
3	41SG27	Disp. Male	18.67	14.39	11.56	6.89	48.77	505.81
3	41SG28	Male	15.50	12.89	11.33	4.17	52.83	557.42
3	41SG29	Male	16.72	13.39	11.78	4.94	48.77	464.52
3	41SG30	Male	16.11	14.28	12.61	3.50	48.77	588.39
3	41SG31	Male	19.11	14.61	12.83	6.28	56.90	701.93
3	41SG32	Male	16.11	13.22	11.83	4.28	60.96	392.26
3	41SG33	Disp. Male	27.56	14.28	12.28	6.00	44.70	567.74
3	41SG34	Male	15.83	14.50	13.50	2.33	48.77	381.93
3	41SG35	Disp. Male	26.61	17.39	13.50	13.11	52.83	867.10
3	41SG36	Male	16.78	14.50	13.39	3.39	48.77	464.52
4	44SG01	Female	13.67	11.33	10.28	3.39	31.24	277.74
4	44SG02	Male	16.33	11.94	10.33	6.00	59.36	650.71
4	44SG03	Disp. Male	32.50	17.56	11.06	18.94	43.74	706.26
4	44SG04	Disp. Male	29.67	12.56	11.06	6.39	43.74	706.26

4	44SG05	Female	13.50	11.33	10.39	3.11	43.74	396.77
4	44SG06	Female	13.39	11.28	10.56	2.83	37.49	404.71
4	44SG07	Disp. Male	30.72	14.94	10.28	19.28	46.86	722.13
4	44SG08	Male	14.94	11.61	10.56	4.39	37.49	468.19
4	44SG09	Male	17.33	12.39	10.78	6.56	46.86	714.19
4	44SG10	Male	15.61	12.56	10.72	4.89	40.61	571.35
4	44SG11	Male	18.39	13.28	11.78	6.61	43.74	539.61
4	44SG12	Male	16.50	12.83	11.28	5.22	43.74	404.71
4	44SG13	Disp. Male	26.94	16.06	12.17	14.78	34.37	634.84
4	44SG14	Disp. Male	30.11	17.06	11.72	18.39	31.24	753.87
4	44SG15	Female	13.61	12.11	10.83	2.78	34.37	341.23
4	44SG16	Disp. Male	27.72	16.56	12.44	12.06	46.86	793.55
4	44SG17	Female	14.22	12.67	11.61	2.61	46.86	452.32
4	44SG18	Male	13.28	9.61	8.28	5.00	49.99	539.61
4	44SG19	Male	15.28	11.06	9.22	6.06	40.61	515.81
4	44SG20	Male	15.89	11.00	8.61	7.28	34.37	579.29
4	44SG21	Male	18.11	13.28	11.56	5.83	34.37	642.77
4	44SG22	Disp. Male	23.78	14.94	11.72	11.72	43.74	682.45
4	45SG23	Female	14.33	12.17	11.17	3.17	40.61	301.55
4	45SG24	Male	17.00	13.39	12.11	4.89	56.24	531.68
4	45SG25	Male	16.33	13.94	12.94	3.39	46.86	380.90
4	45SG26	Disp. Male	26.94	15.11	13.39	5.78	37.49	507.87
4	45SG27	Male	17.33	14.61	12.94	4.39	46.86	412.64
4	45SG28	Disp. Male	26.89	18.06	13.11	13.78	37.49	603.10
4	45SG29	Male	18.94	16.28	13.89	5.06	46.86	626.90
4	45SG30	Female	15.44	13.78	13.06	2.39	31.24	333.29
5	46SG01	Male	19.50	15.00	12.56	6.94	56.24	666.58
5	46SG02	Male	18.28	14.39	12.89	5.39	46.86	452.32
5	46SG03	Disp. Male	27.17	15.56	13.44	6.22	46.86	698.32
5	46SG04	Female	16.17	14.17	13.06	3.11	34.37	357.10
5	46SG05	Male	17.56	14.28	12.89	4.67	37.49	301.55
5	46SG06	Disp. Male	32.44	20.17	13.44	19.00	40.61	714.19
5	46SG07	Disp. Male	30.44	19.94	14.33	16.11	37.49	738.00
5	46SG08	Disp.	19.72	15.94	13.61	6.11	37.49	650.71

		Male						
5	46SG09	Male	16.28	13.72	12.44	3.83	31.24	444.39
5	46SG10	Male	16.61	13.50	11.67	4.94	53.11	611.03
5	46SG11	Disp.	31.11	18.94	13.33	17.78	34.37	611.03
		Male						
5	46SG12	Female	16.00	13.94	12.72	3.28	43.74	349.16
5	46SG13	Disp.	25.89	17.33	13.11	12.78	31.24	626.90
		Male						
5	46SG14	Male	17.61	14.11	12.67	4.94	34.37	587.22
5	46SG15	Male	19.89	13.22	10.94	8.94	46.86	587.22
5	46SG16	Male	16.94	12.61	11.22	5.72	49.99	563.42
5	46SG17	Male	17.78	13.56	11.72	6.06	46.86	468.19
5	46SG23	Female	14.00	15.28	10.94	3.06	34.37	428.52
5	47SG18	Female	11.94	10.17	8.50	3.44	34.37	412.64
5	47SG19	Female	15.00	12.83	11.67	3.33	40.61	420.58
5	47SG20	Male	17.56	15.06	12.56	5.00	46.86	499.93
5	47SG21	Male	18.61	13.78	11.89	6.72	49.99	587.22
5	47SG22	Disp.	28.28	18.67	13.11	15.17	43.74	634.84
		Male						

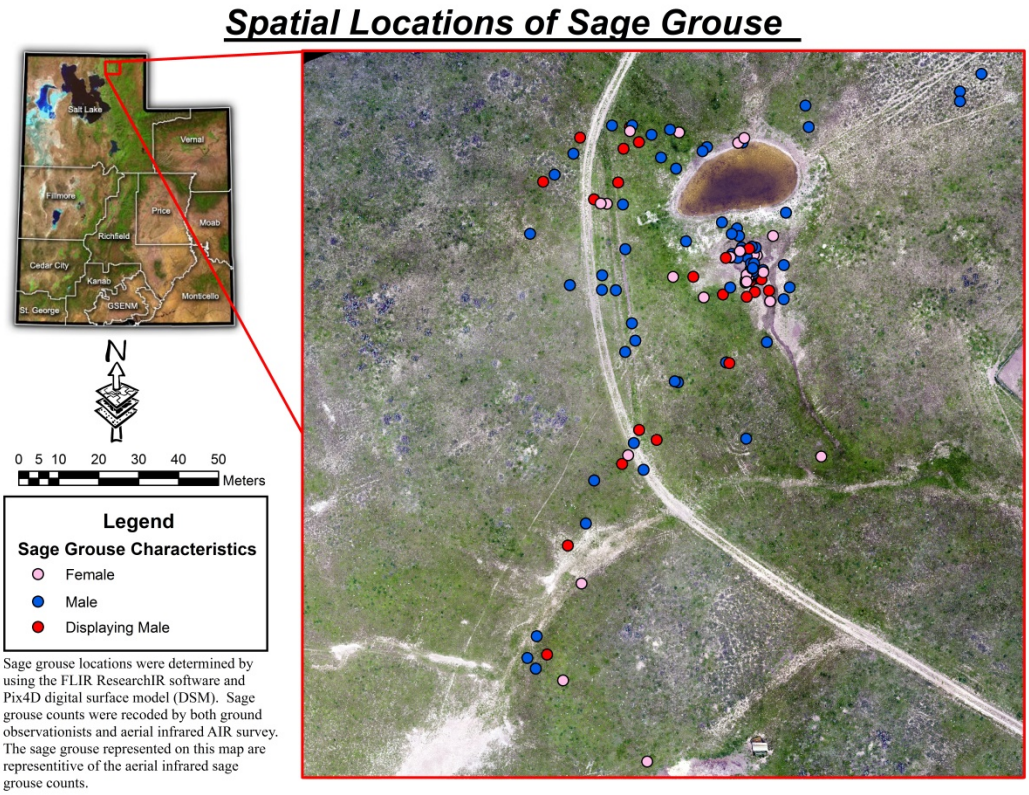

Figure A-1 The spatial disribution of the sage-grouse in this map this map is representative of the ae sage groue observed during the aerial survey.

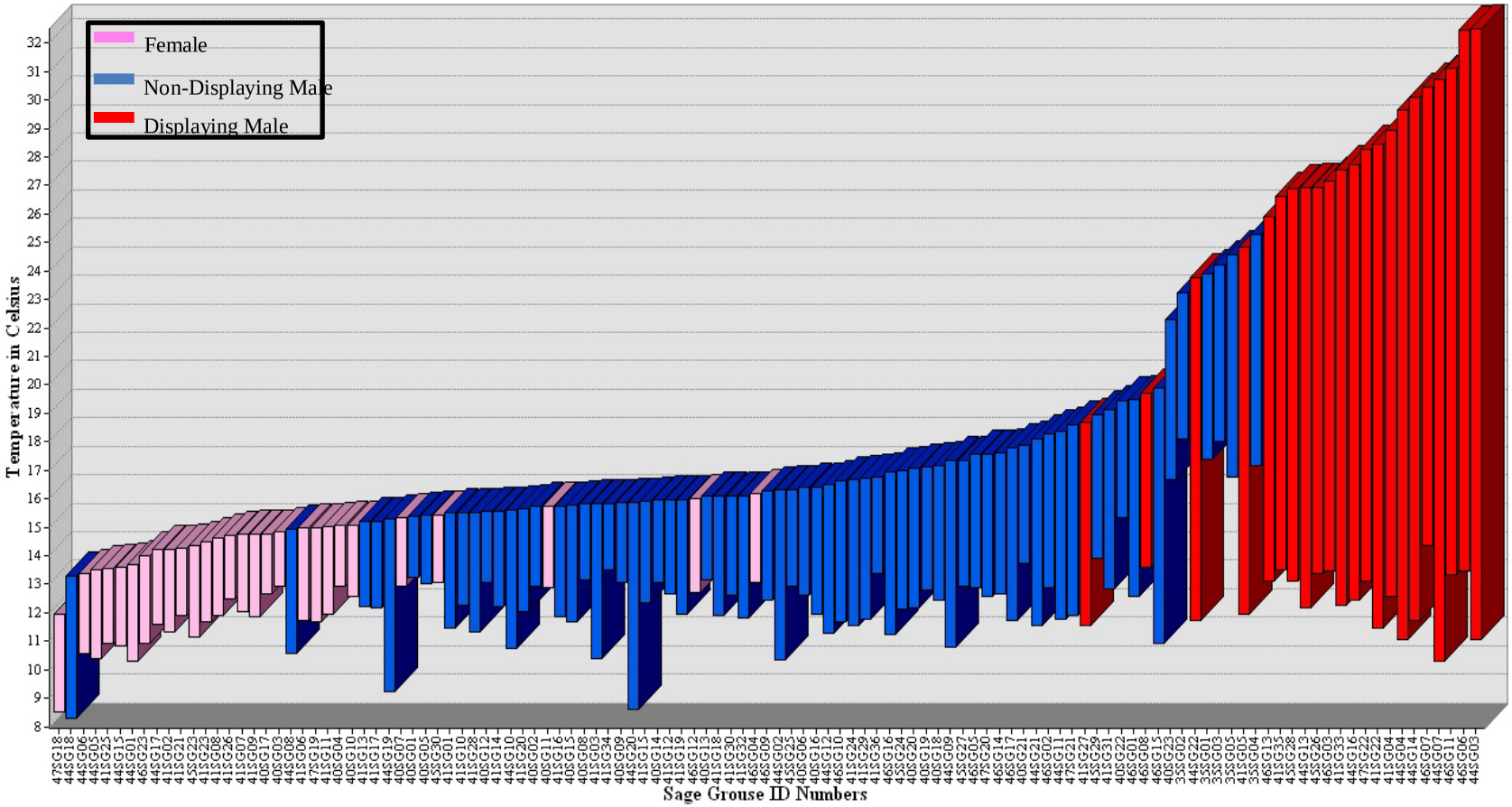

Figure A-2 The bars in the graph are the Displaying Males, blue bars are the Non-Displaying Males, and the pink bars are the Females. All individuals were classified based on three metrics: maximum temperature, range of temprature, and size of sage-grouse (Table 4). Sage-grouse temperature samples were taken from the rasterized thermal data and the minimum temperature was subtracted from the maximum temperature value to deduce the range of temperature value.

Figure A-3 to A-89 These figures demonstrate the measurable thermographic response measured using a FLIR A65sc 640x512 25mm camera mounted to a DJI s1000 remotely piloted aircraft (RPA). The thermal camera being used is an uncooled microbolometer detector for, specializing in measuring longwave infrared energy. The FLIR ResearchIR software generated all of the thermographic images and transect profiles plots.

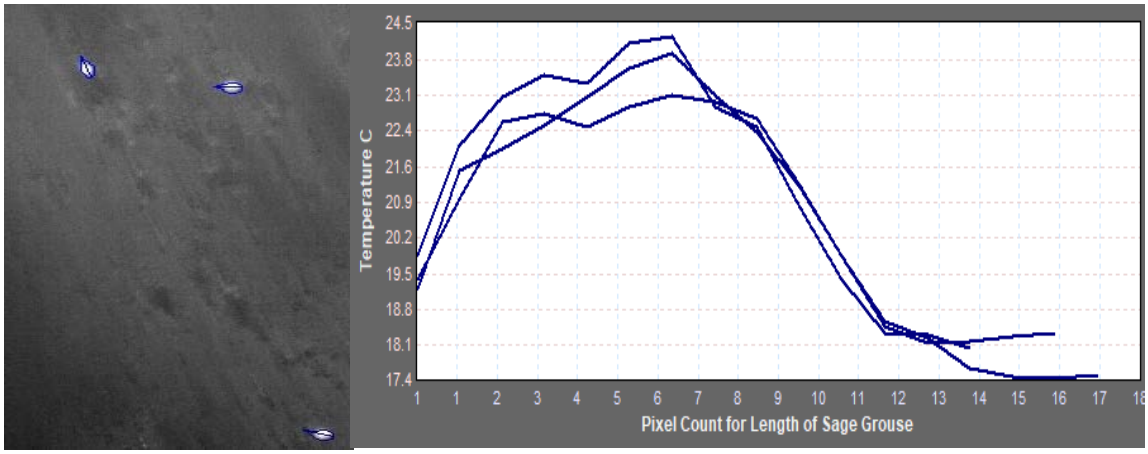

Figure A-3. Thermographic Data for (03-05-2016) Flight 1 Record 35: sage-grouse individuals 01-03. The non displaying males are represented by the blue transects.

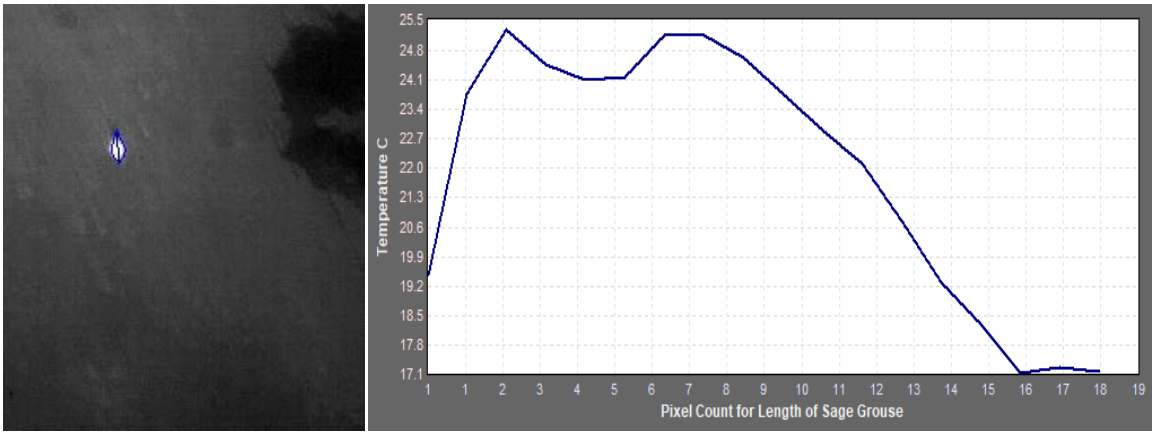

Figure A-4. Thermographic Data for (03-05-2016) Flight 1 Record 35: sage-grouse individual 04. The non displaying male is represented by the blue transect.

Figure A-5. Thermographic Data for (03-05-2016) Flight 1 Record 35: sage-grouse individual 05. The non displaying male is represented by the blue transect.

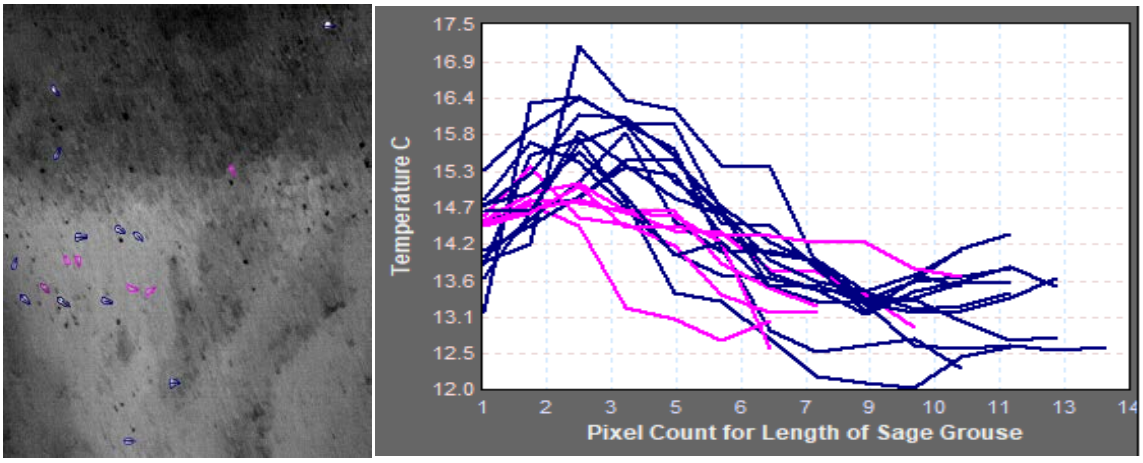

Figure A-6. Thermographic Data for (03-12-2016) Flight 2 Record 40: sage-grouse individuals 01–18. Females are represented by the pink transects and the non displaying males are represented by the blue transects.

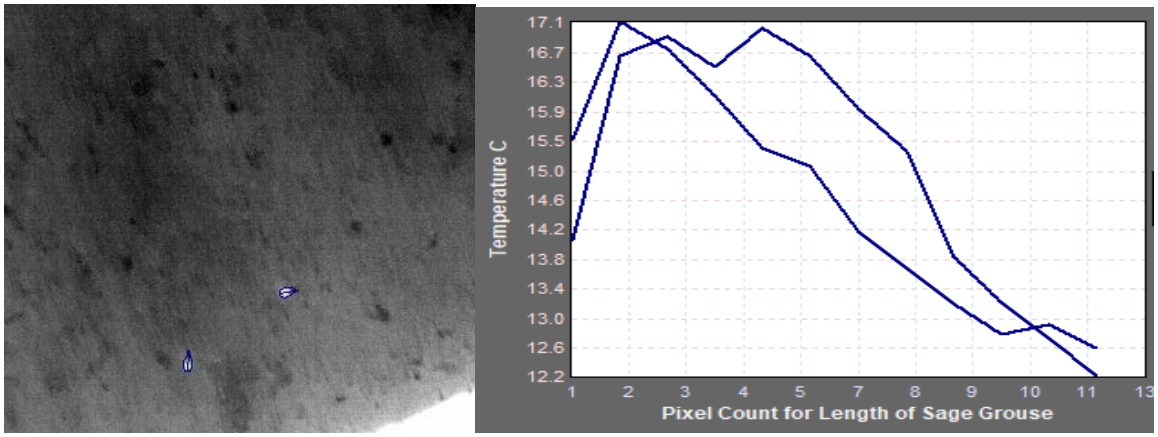

Figure A-7. Thermographic Data for (03-12-2016) Flight 2 Record 40: sage-grouse individuals 19 – 20. The non displaying males are represented by the blue transects.

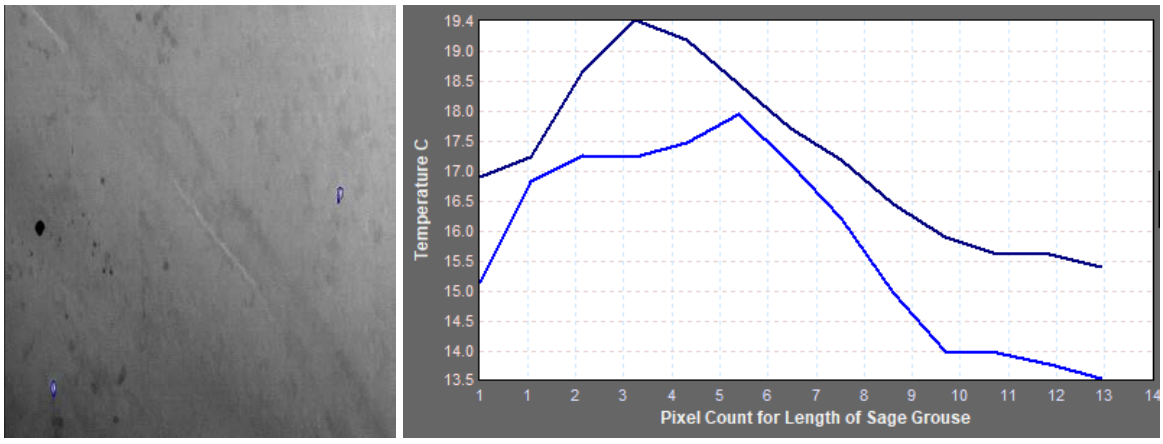

Figure A-8. Thermographic Data for (03-12-2016) Flight 2 Record 40: sage-grouse individuals 21 – 22. The non displaying males are represented by the blue transects.

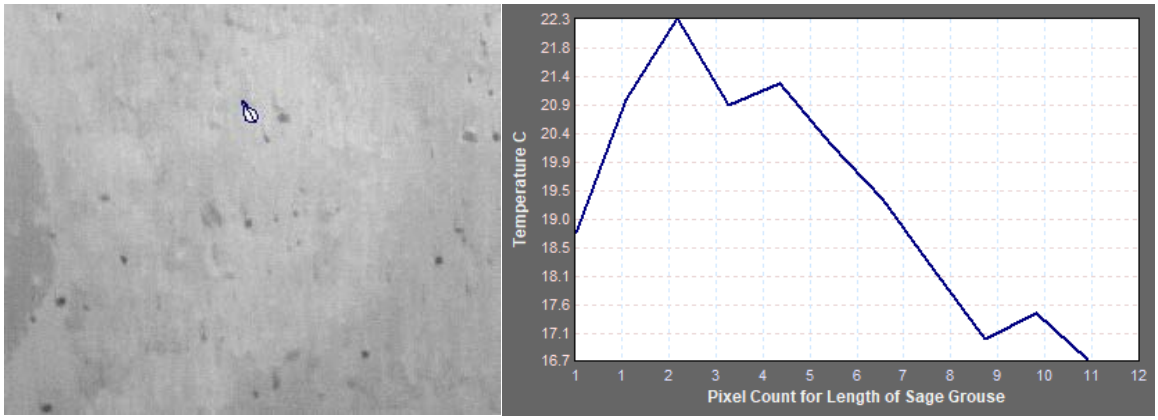

Figure A-9. Thermographic Data for (03-12-2016) Flight 2 Record 40: sage-grouse individual 23 The non displaying male is represented by the blue transect.

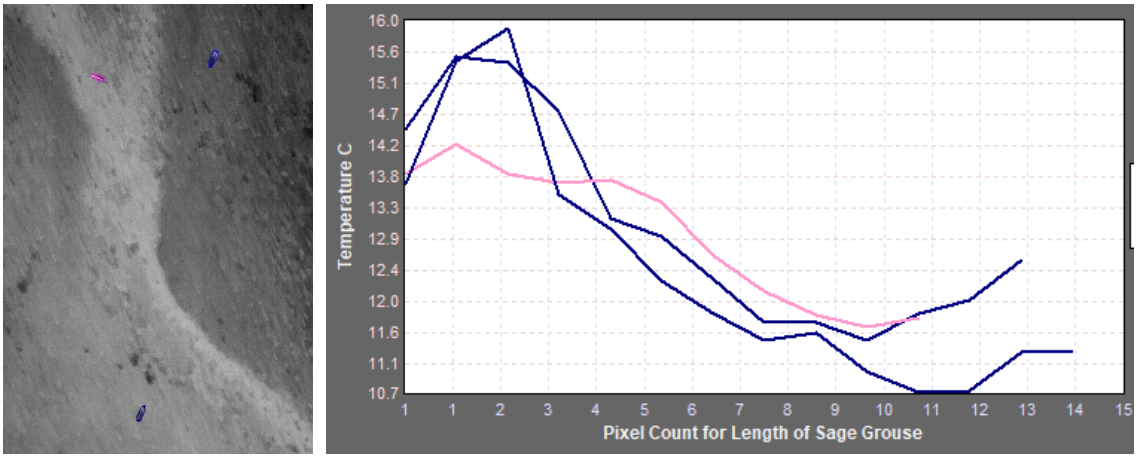

Figure A-10. Thermographic Data for (03-26-2016) Flight 3 Record 41: sage-grouse individuals 01-03. Females are represented by the pink transects and the non displaying males are represented by the blue transects.

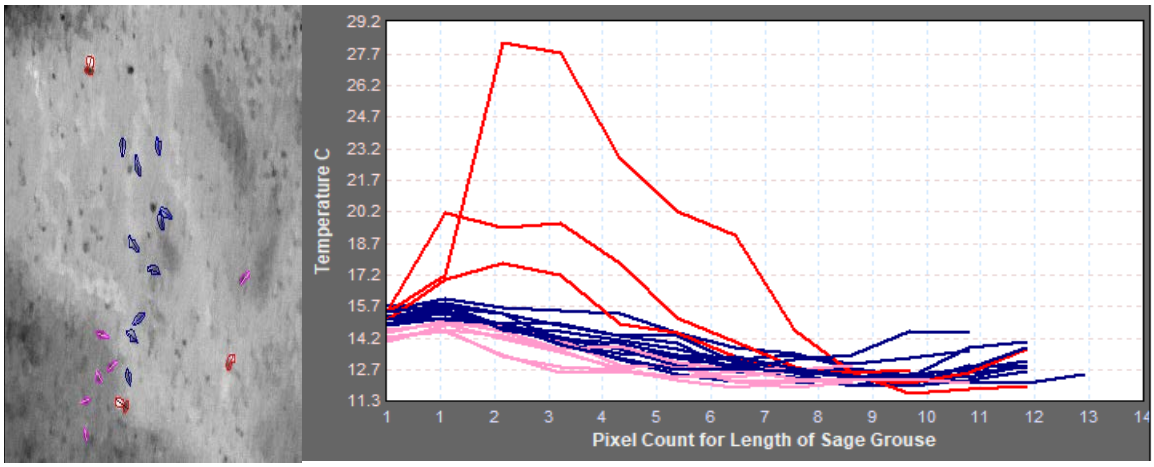

Figure A-11. Thermographic Data for (03-26-2016) Flight 3 Record 41: sage-grouse individuals 04-22. Females are represented by the pink transects and the non displaying males are represented by the blue transects the males that were observed displaying with the thermal sensor were classified as displaying males are indicated by the red transect line.

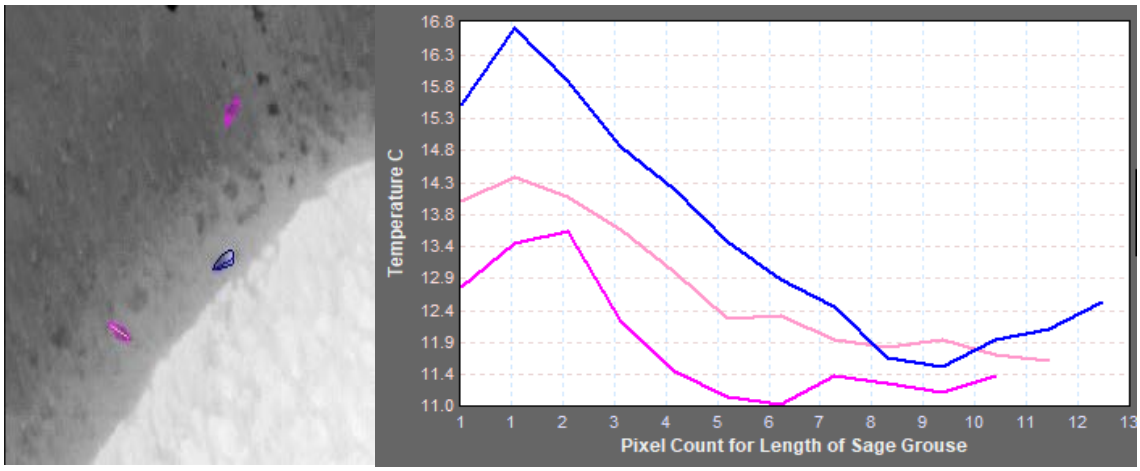

Figure A-12. Thermographic Data for (03-26-2016) Flight 3 Record 41: sage-grouse individuals 23-25. Females are represented by the pink transects and the non displaying males are represented by the blue transects.

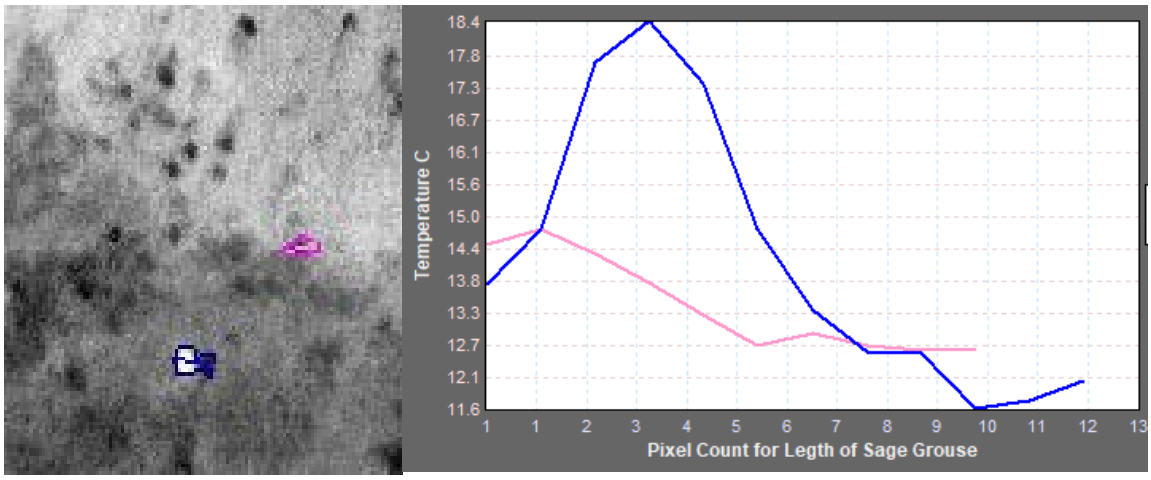

Figure A-13. Thermographic Data for (03-26-2016) Flight 3 Record 41: sage-grouse individuals 26-27. Females are represented by the pink transects and the non displaying males are represented by the blue transects.

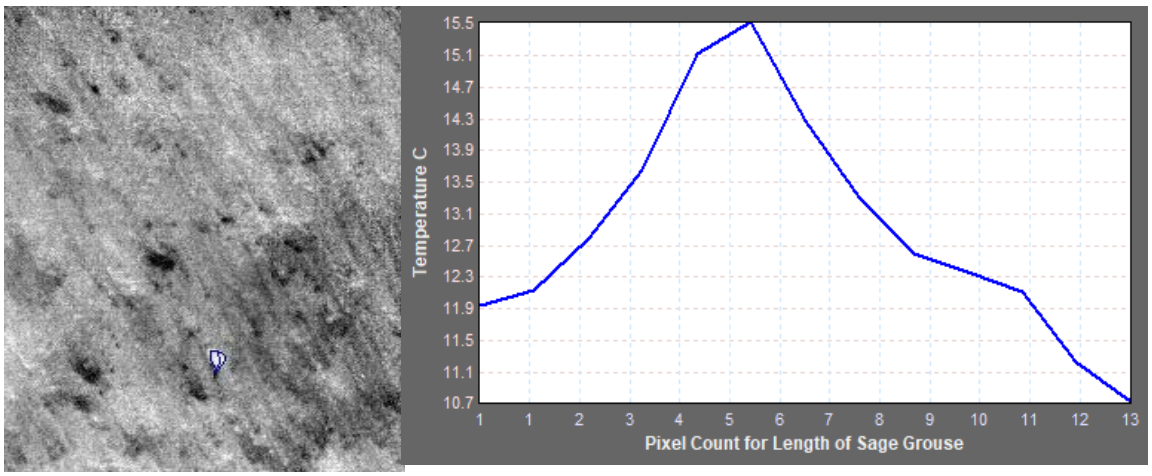

Figure A-14. Thermographic Data for (03-26-2016) Flight 3 Record 41: sage-grouse individual 28. The non displaying male is represented by the blue transect.

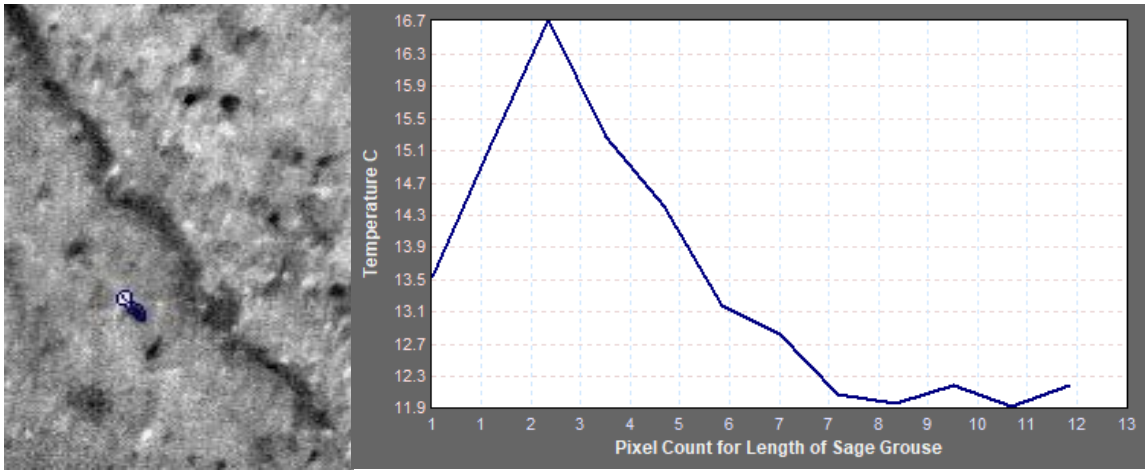

Figure A-15. Thermographic Data for (03-26-2016) Flight 3 Record 41: sage-grouse individual 29. The non displaying male is represented by the blue transect.

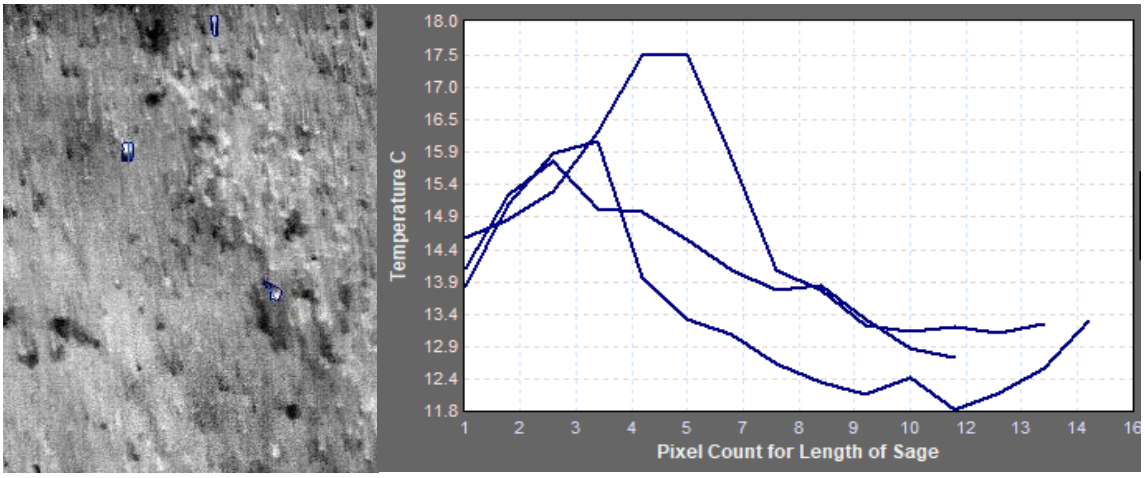

Figure A-16. Thermographic Data for (03-26-2016) Flight 3 Record 41: sage-grouse individuals 30-32. The non displaying males are represented by the blue transects.

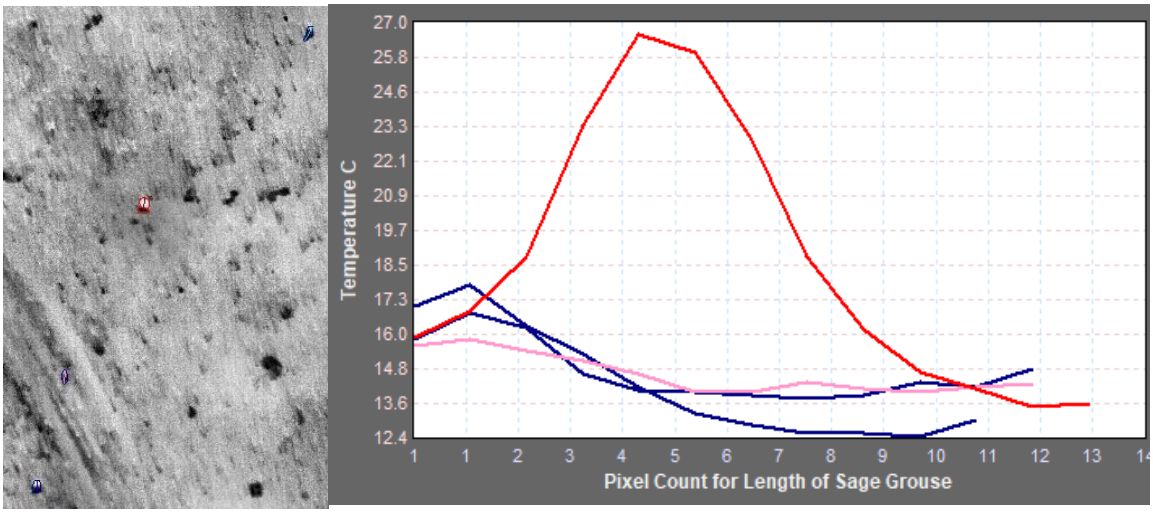

Figure A-17. Thermographic Data for (03-26-2016) Flight 3 Record 41: sage-grouse individuals33-36. Females are represented by the pink transects and the non displaying males are represented by the blue transects and the males that were observed displaying with the thermal sensor were classified as displaying males are indicated by the red transect line.

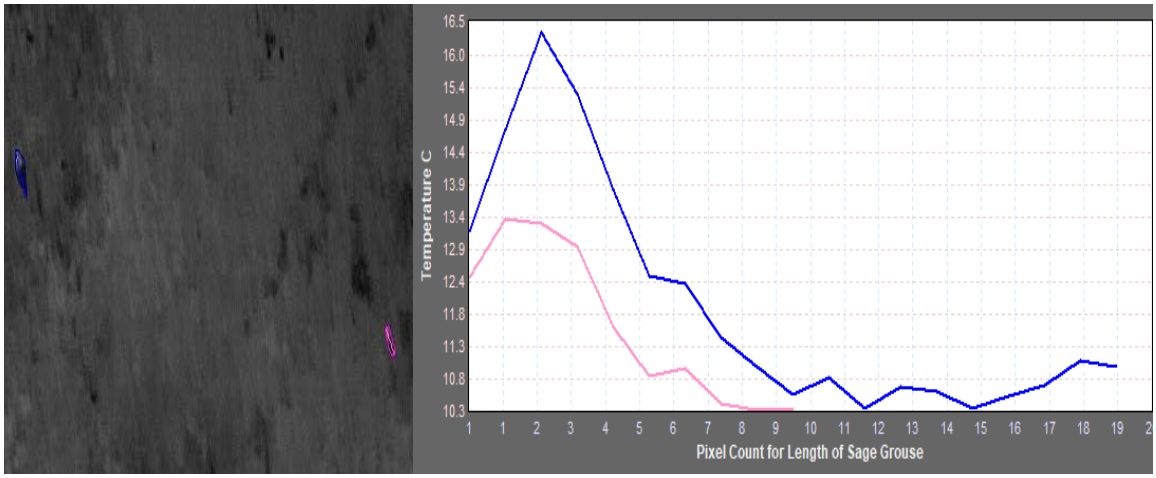

Figure A-18. Thermographic Data for (04-02-2016) Flight 4 Record 44: sage-grouse individuals 01-02. Females are represented by the pink transects and the non displaying males are represented by the blue transects.

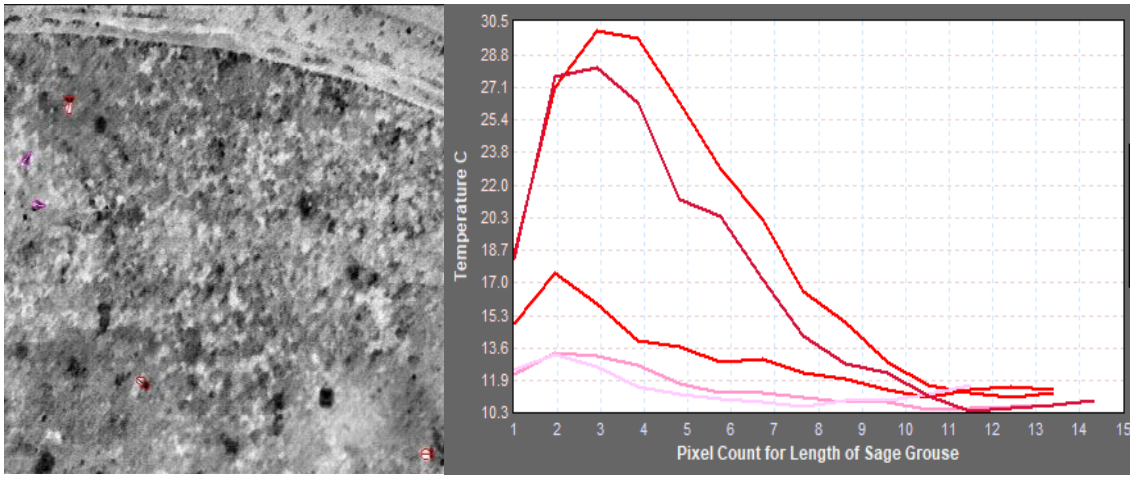

Figure A-19. Thermographic Data for (04-02-2016) Flight 4 Record 44: sage-grouse individuals 03-07. Females are represented by the pink transects and the males that were observed displaying with the thermal sensor were classified as displaying males are indicated by the red transect line.

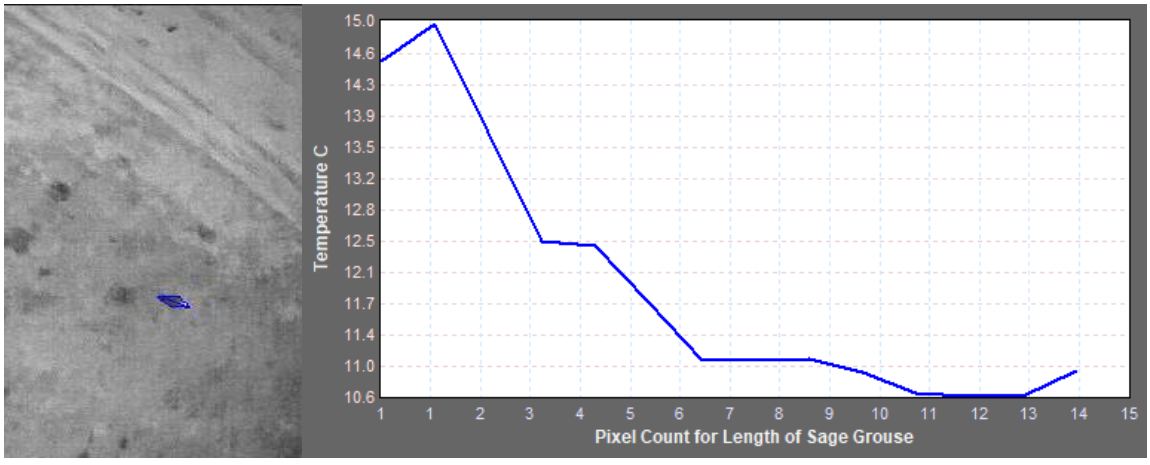

Figure A-20. Thermographic Data for (04-02-2016) Flight 4 Record 44: sage-grouse individual 08. The non displaying male is represented by the blue transect.

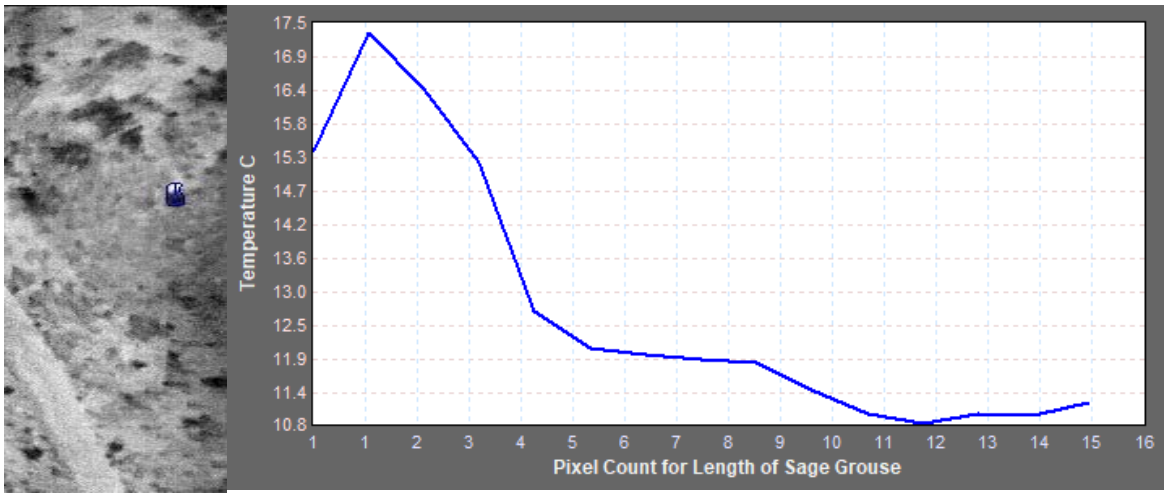

Figure A-21. Thermographic Data for (04-02-2016) Flight 4 Record 44: sage-grouse individual 09. The non displaying male is represented by the blue transect.

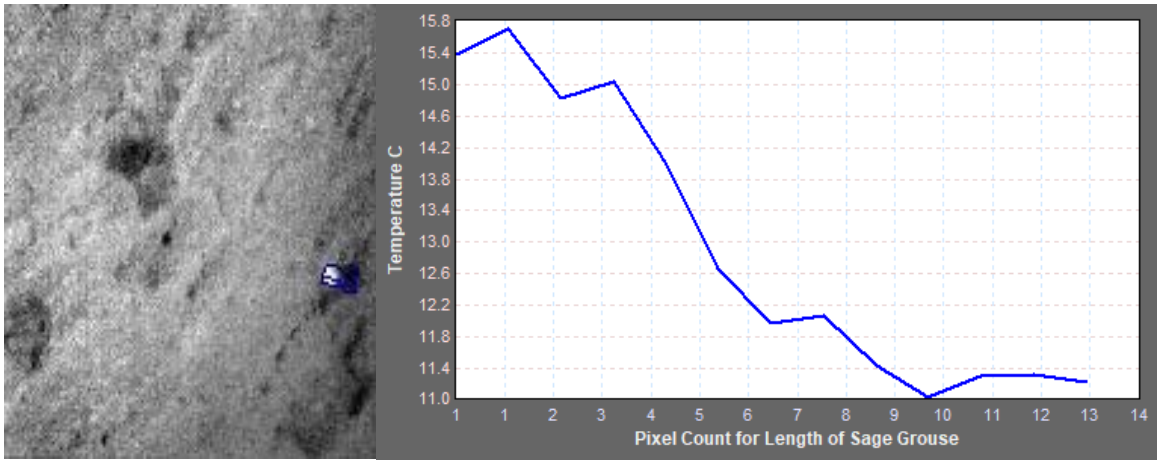

Figure A-22. Thermographic Data for (04-02-2016) Flight 4 Record 44: sage-grouse individual 10. The non displaying male is represented by the blue transect.

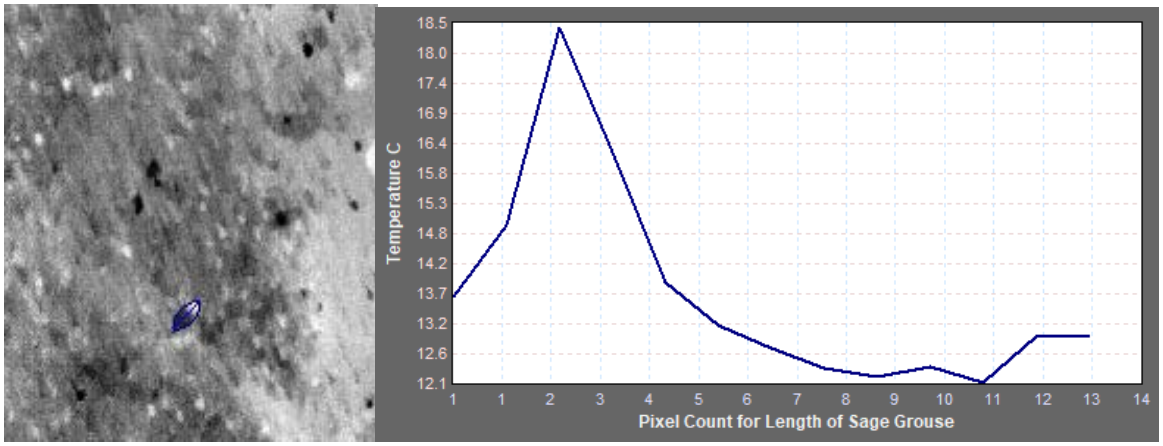

Figure A-23. Thermographic Data for (04-02-2016) Flight 4 Record 44: sage-grouse individual 11. The non displaying male is represented by the blue transect.

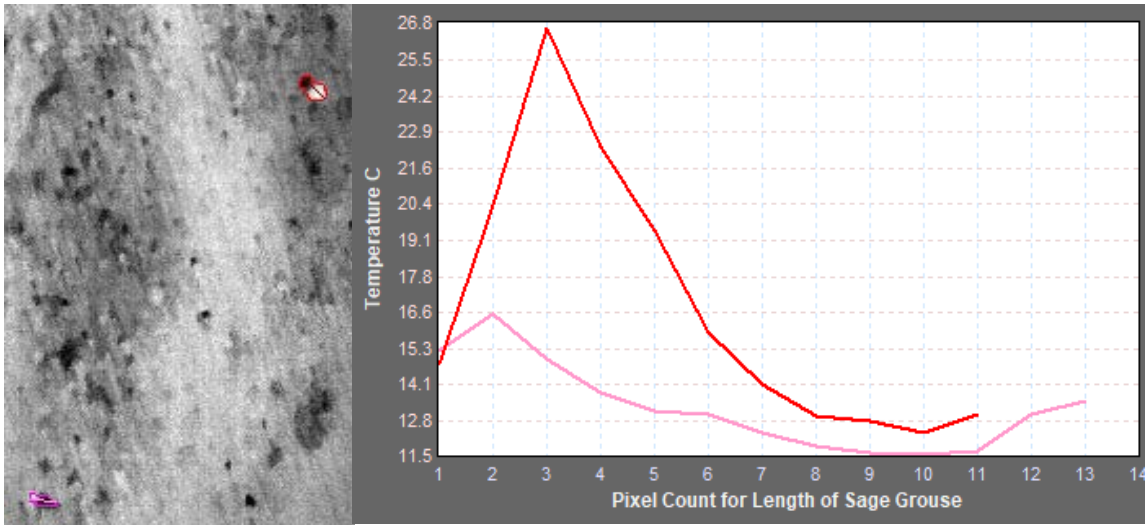

Figure A-24. Thermographic Data for (04-02-2016) Flight 4 Record 44: sage-grouse individuals 12-13. This female is represented by the pink transects and the displaying male is indicated by the red transect line.

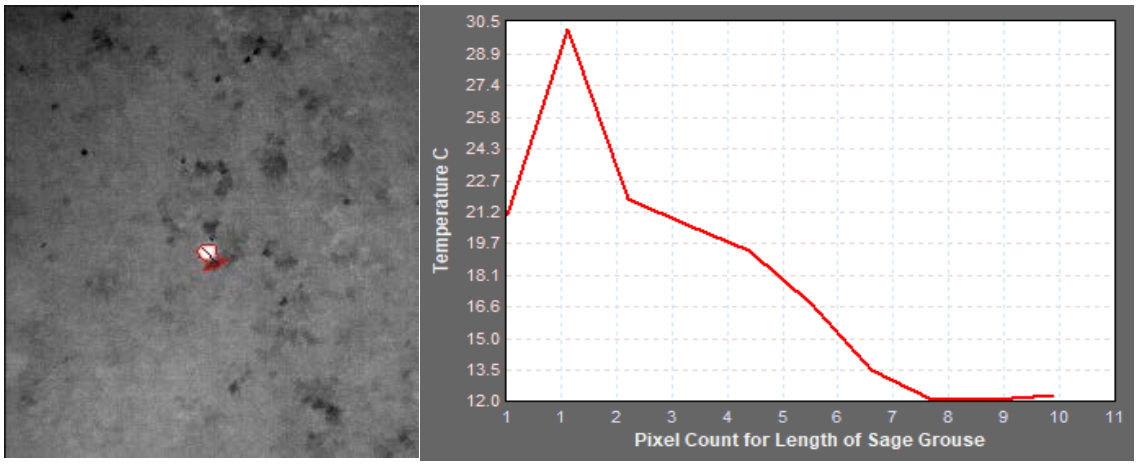

Figure A-25. Thermographic Data for (04-02-2016) Flight 4 Record 44: sage-grouse individual 14. The red transect line indicates the displaying male temperature profile.

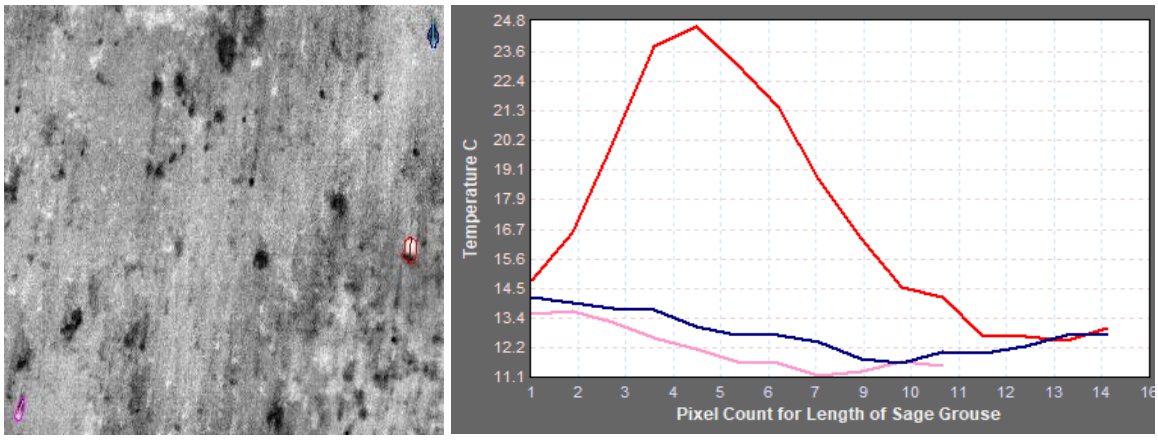

Figure A-26. Thermographic Data for (04-02-2016) Flight 4 Record 44: sage-grouse individuals 15-17. Females are represented by the pink transects and the non displaying males are represented by the blue transects and the males that were observed displaying with the thermal sensor were classified as displaying males are indicated by the red transect line.

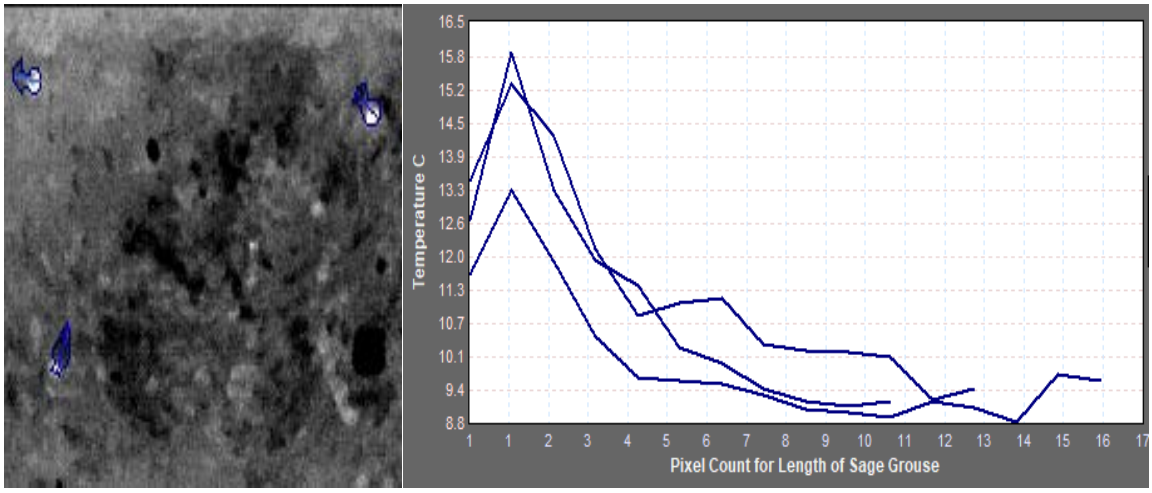

Figure A-27. Thermographic Data for (04-02-2016) Flight 4 Record 44: sage-grouse individuals 18-20. The non displaying males are represented by the blue transects.

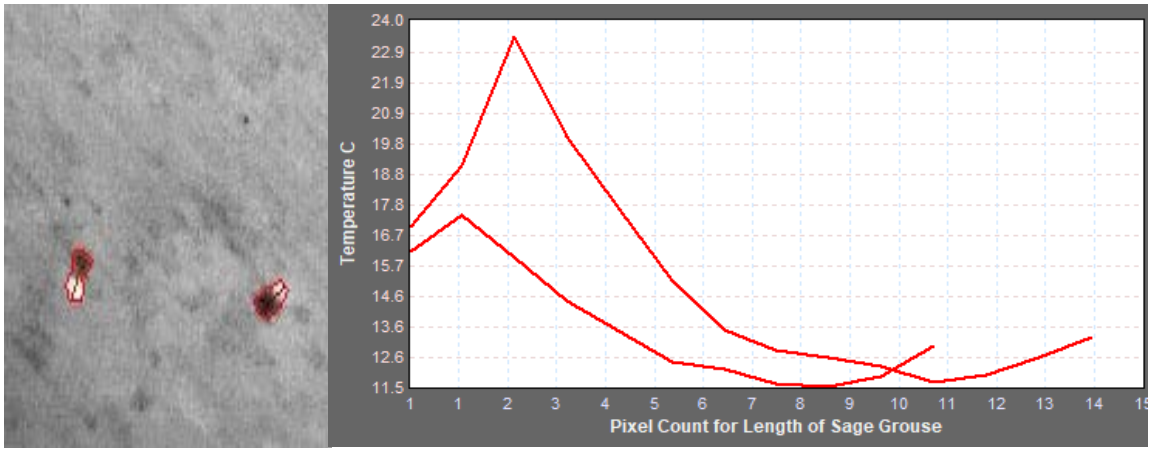

Figure A-28. Thermographic Data for (04-02-2016) Flight 4 Record 44: sage-grouse individuals 21-22. Displaying males are indicated by the red transect lines.

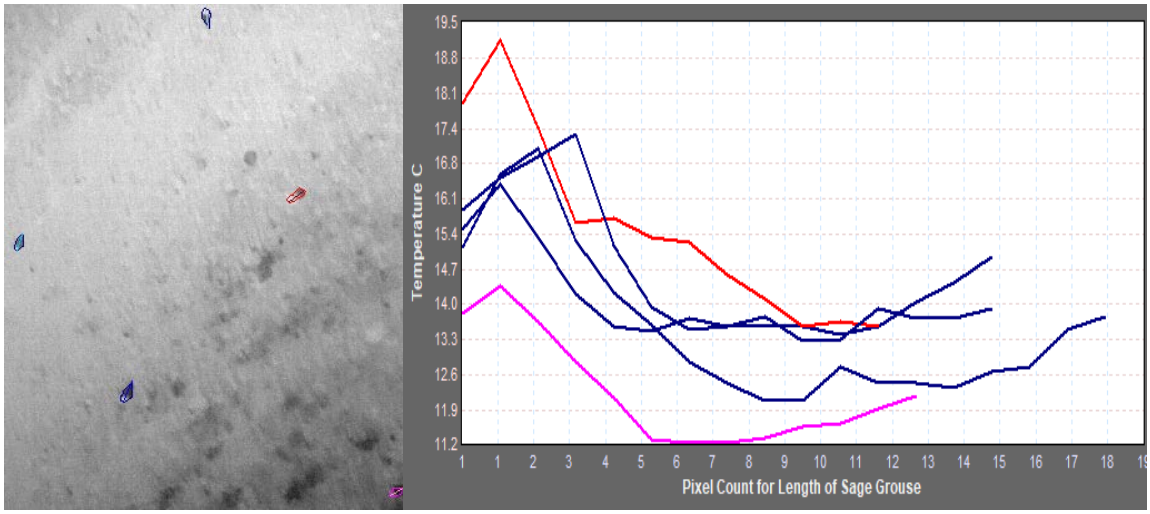

Figure A-29. Thermographic Data for (04-02-2016) Flight 4 Record 44: sage-grouse individuals 23-27. Females are represented by the pink transects and the non displaying males are represented by the blue transects and the males that were observed displaying with the thermal sensor were classified as displaying males are indicated by the red transect line.

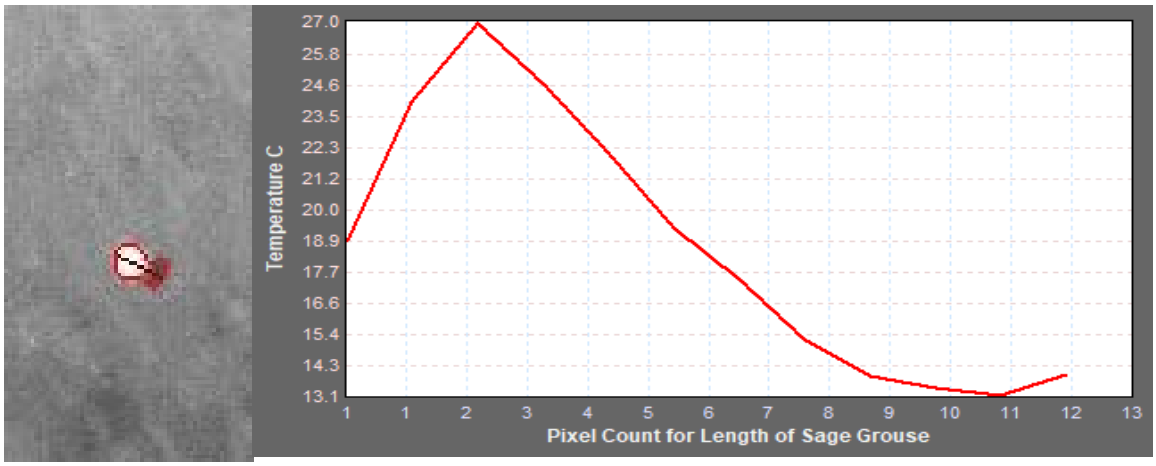

Figure A-30. Thermographic Data for (04-02-2016) Flight 4 Record 45: sage-grouse individual 28. This Displaying male is indicated by the red transect line.

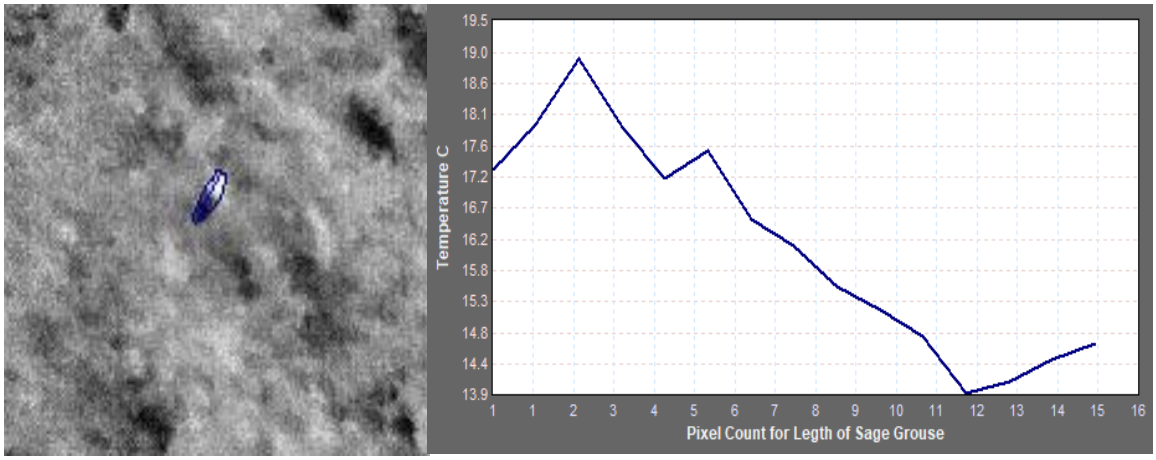

Figure A-31. Thermographic Data for (04-02-2016) Flight 4 Record 45: sage-grouse individual 29. The non displaying male is represented by the blue transect.

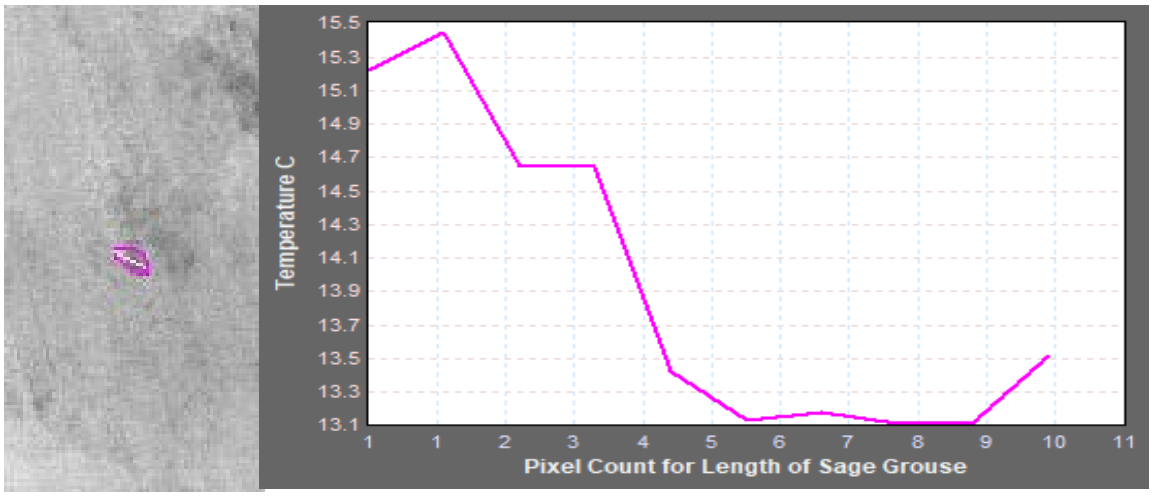

Figure A-32. Thermographic Data for (04-02-2016) Flight 4 Record 45: sage-grouse individual 30. Females are represented by the pink transects.

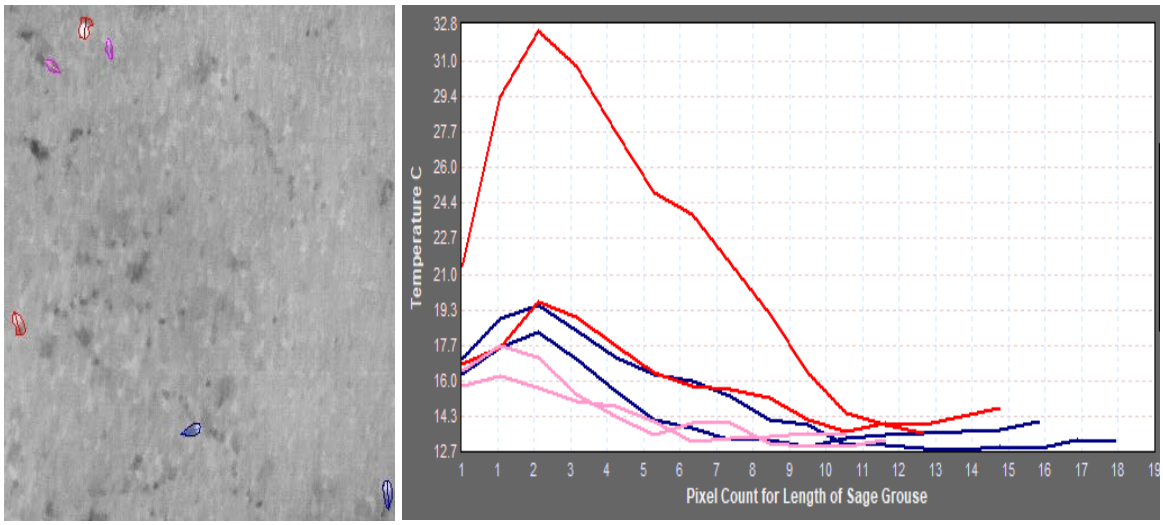

Figure A-33. Thermographic Data for (04-05-2016) Flight 5 Record 46: sage-grouse individuals 01-06. Females are represented by the pink transects and the non displaying males are represented by the blue transects and the males that were observed displaying with the thermal sensor were classified as displaying males are indicated by the red transect line.

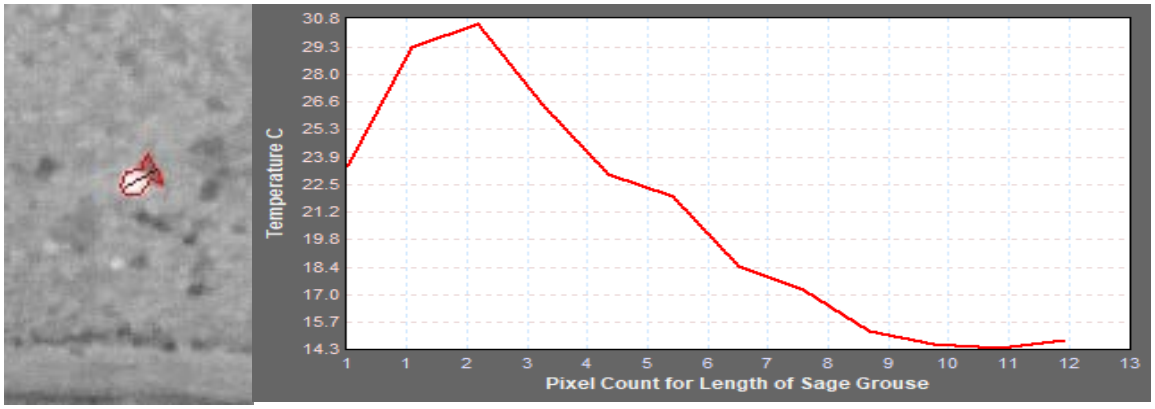

Figure A-34. Thermographic Data for (04-05-2016) Flight 5 Record 46: sage-grouse individual 07. This Displaying is indicated by the red transect line.

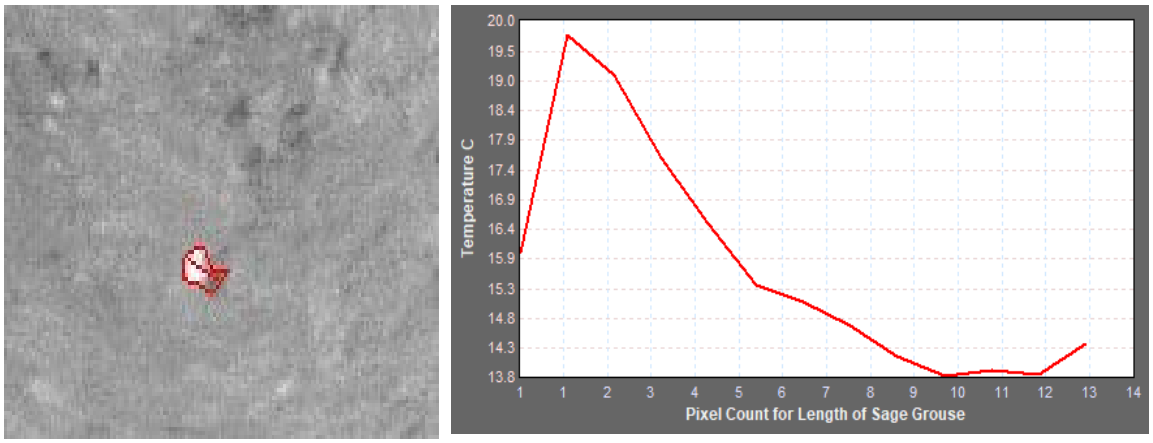

Figure A-35. Thermographic Data for (04-05-2016) Flight 5 Record 46: sage-grouse individual 08. Again, this displaying male is indicated by the red transect line.

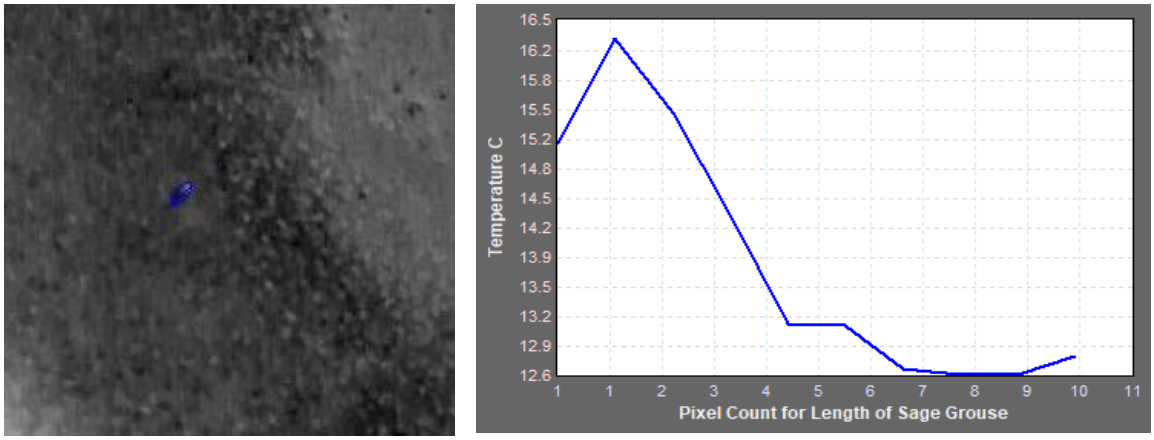

Figure A-36. Thermographic Data for (04-05-2016) Flight 5 Record 46: sage-grouse individual 09. Females are represented by the pink transects.

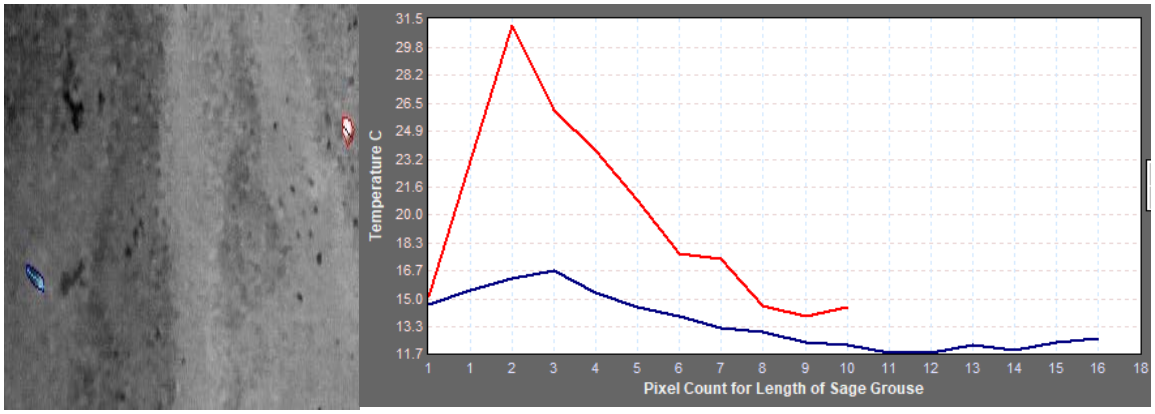

Figure A-37. Thermographic Data for (04-05-2016) Flight 5 Record 46: sage-grouse individuals 10-11. The non displaying male is represented by the blue transect and the displaying male is indicated by the red transect line.

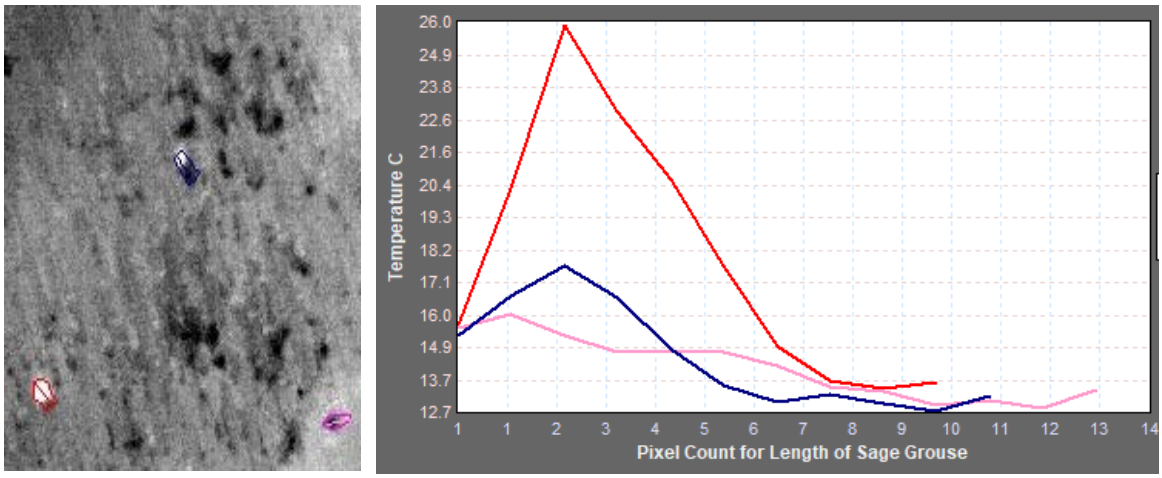

Figure A-38. Thermographic Data for (04-05-2016) Flight 5 Record 46: sage-grouse individuals 01-06. Females are represented by the pink transects and the non displaying males are represented by the blue transects and the males that were observed displaying with the thermal sensor were classified as displaying males are indicated by the red transect line.

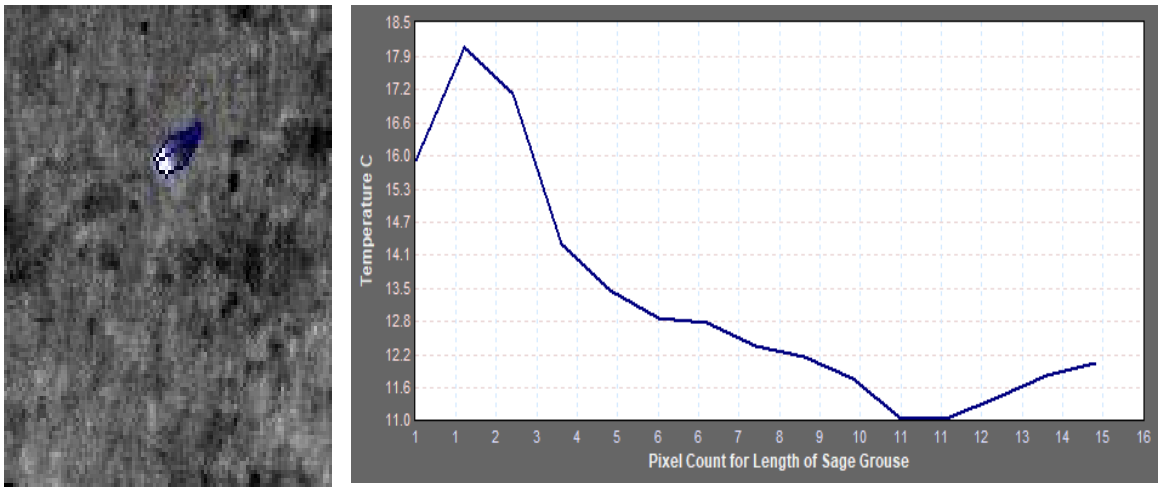

Figure A-39. Thermographic Data for (04-05-2016) Flight 5 Record 46: sage-grouse individual 15. The non displaying male is represented by the blue transect.

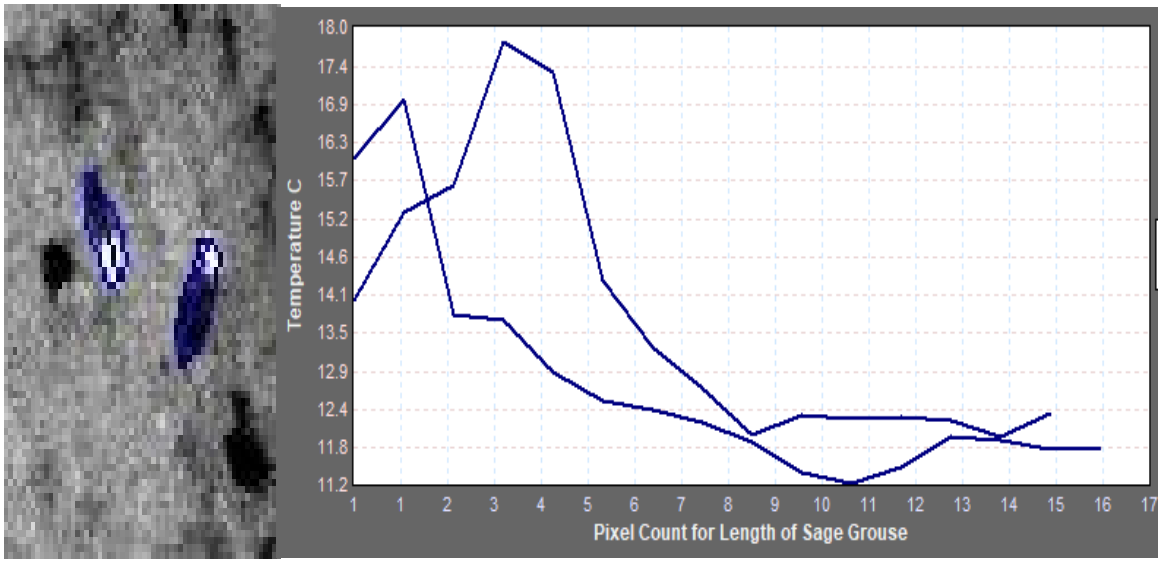

Figure A-40. Thermographic Data for (04-05-2016) Flight 5 Record 46: sage-grouse individuals 16-17. The non displaying males are represented by the blue transects.

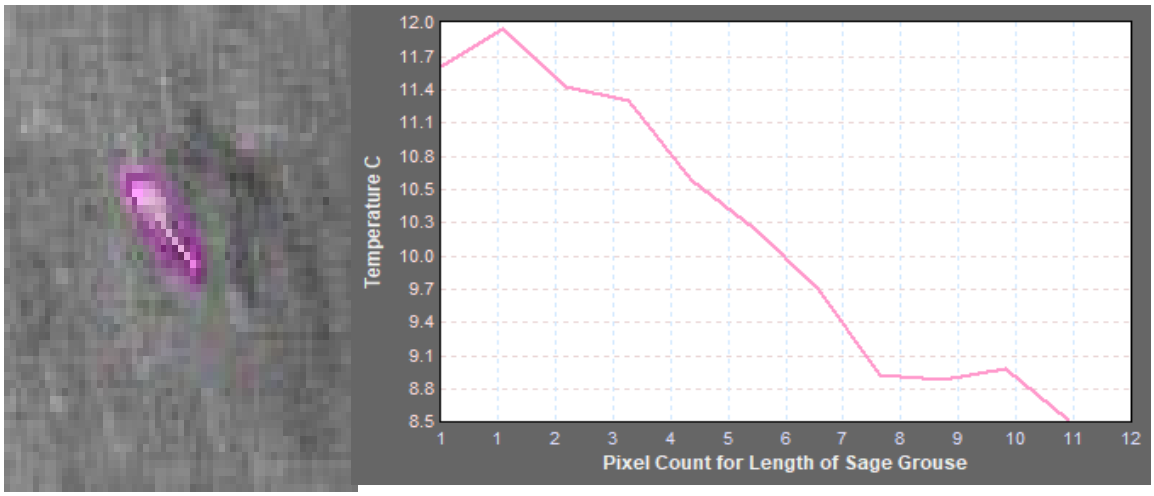

Figure A-41. Thermographic Data for (04-05-2016) Flight 5 Record 46: sage-grouse individuals 18. This Female is represented by the pink transect.

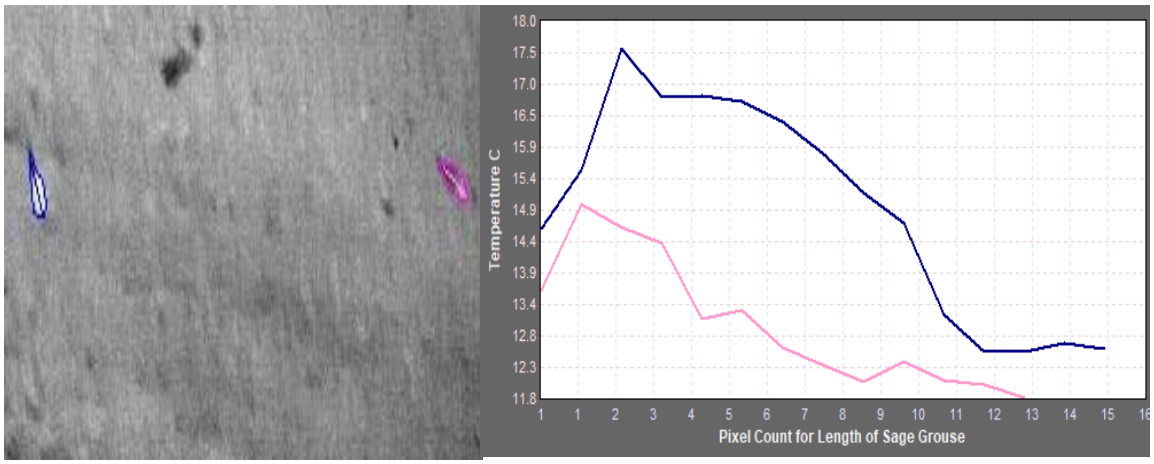

Figure A-42. Thermographic Data for (04-05-2016) Flight 5 Record 46: sage-grouse individuals 19-20. Females are represented by the pink transects and the non displaying males are represented by the blue transects.

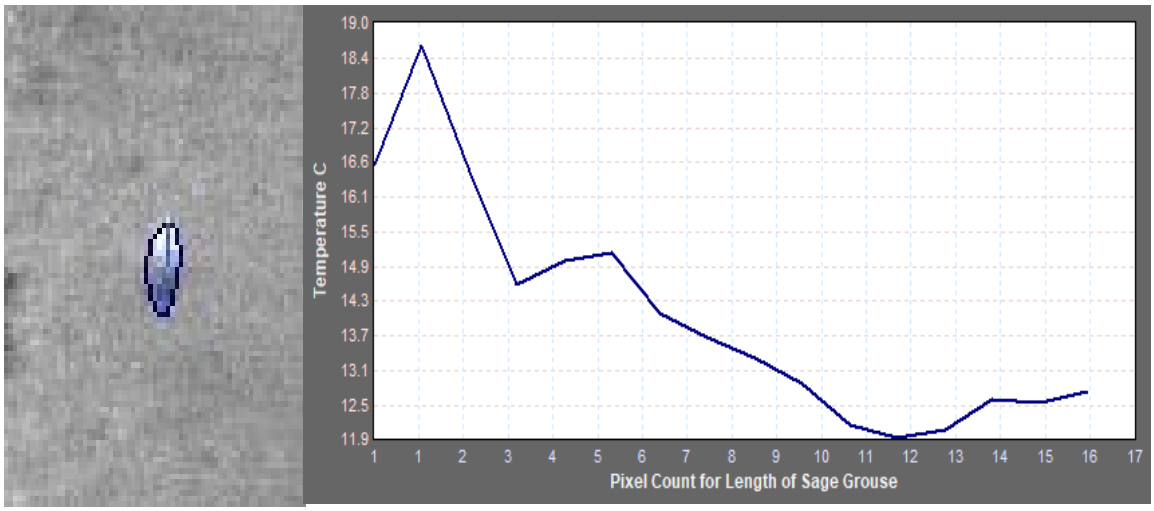

Figure A-43. Thermographic Data for (04-05-2016) Flight 5 Record 46: sage-grouse individual 21. The non displaying male is represented by the blue transect.

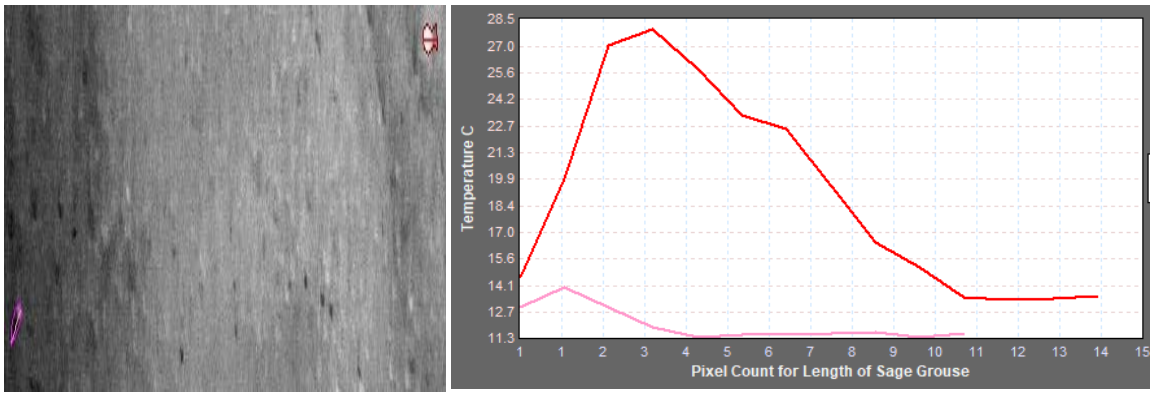

Figure A-44. Thermographic Data for (04-05-2016) Flight 5 Record 46: sage-grouse individuals 22-23. This female is represented by the pink transects and the displaying male is indicated by the red transect line.

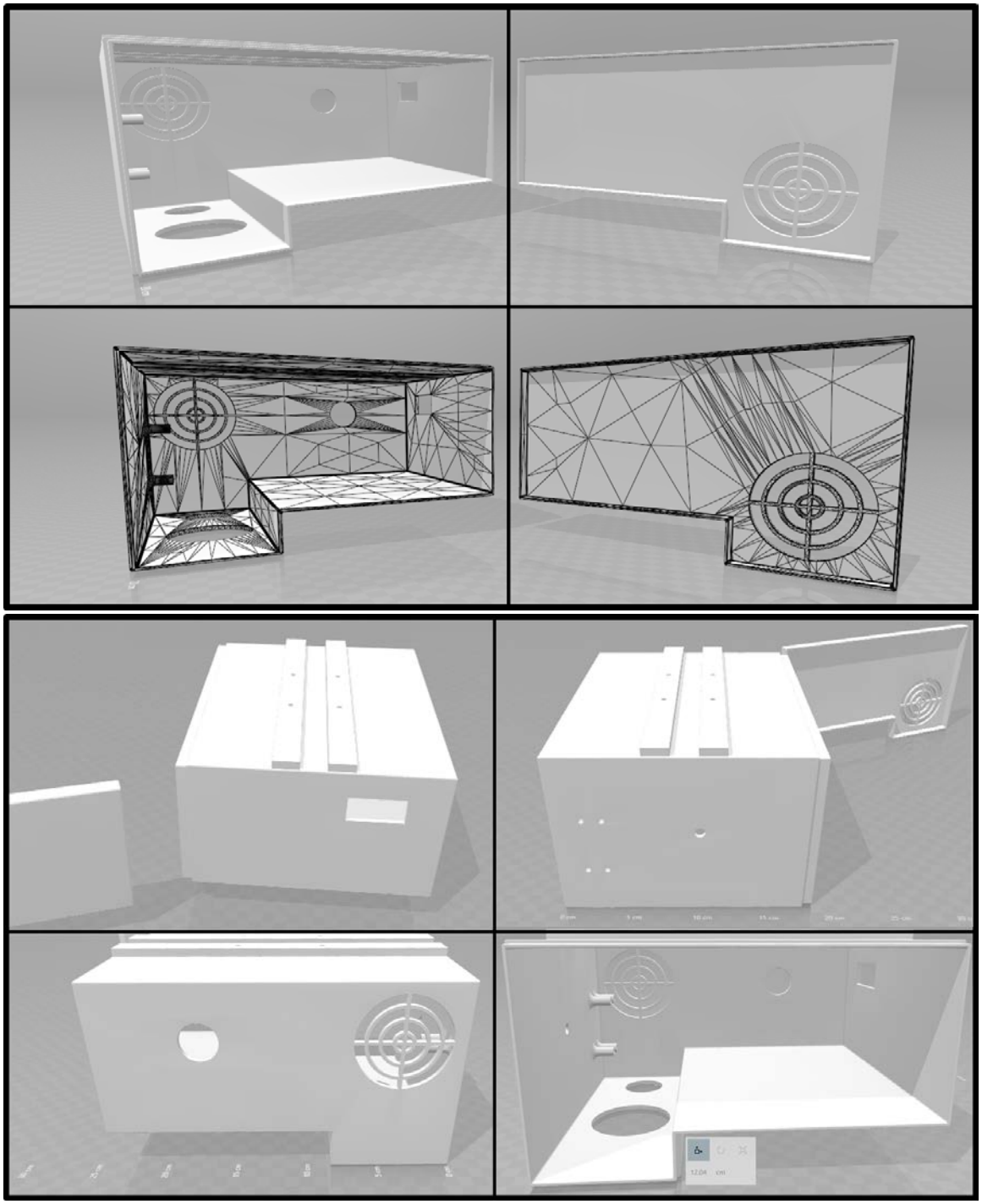

Figure A-45. Design layout for themal camera enclosure..